PLOS ONE

RESEARCH ARTICLE

How conspicuous are peacock eyespots and other colorful feathers in the eyes of mammalian predators?

Suzanne Amador Kane[1]*, Yuchao Wang[1], Rui Fang[1], Yabin Lu[1], Roslyn Dakin[2]

1 Physics & Astronomy Department, Haverford College, Haverford, Pennsylvania, United States of America, **2** Migratory Bird Center, Smithsonian Conservation Biology Institute, National Zoological Park, Washington DC, United States of America

* samador@haverford.edu

OPEN ACCESS

Citation: Kane SA, Wang Y, Fang R, Lu Y, Dakin R (2019) How conspicuous are peacock eyespots and other colorful feathers in the eyes of mammalian predators? PLoS ONE 14(4): e0210924. https://doi.org/10.1371/journal.pone.0210924

Editor: Matthew Shawkey, University of Akron, UNITED STATES

Received: January 3, 2019

Accepted: March 28, 2019

Published: April 24, 2019

Data Availability Statement: All relevant data are within the manuscript, Supporting Information files, and posted at https://figshare.com/s/688fb19dad98b6273324.

Funding: This work was supported by: SAK, RF, YL, YW: Haverford College, www.haverford.edu; RD: National Sciences and Engineering Research Council of Canada (NSERC), Postdoctoral Fellowship, www.nserc-crsng.gc.ca. The funders had no role in study design, data collection and

Abstract

Colorful feathers have long been assumed to be conspicuous to predators, and hence likely to incur costs due to enhanced predation risk. However, many mammals that prey on birds have dichromatic visual systems with only two types of color-sensitive visual receptors, rather than the three and four photoreceptors characteristic of humans and most birds, respectively. Here, we use a combination of multispectral imaging, reflectance spectroscopy, color vision modelling and visual texture analysis to compare the visual signals available to conspecifics and to mammalian predators from multicolored feathers from the Indian peacock (*Pavo cristatus*), as well as red and yellow parrot feathers. We also model the effects of distance-dependent blurring due to visual acuity. When viewed by birds against green vegetation, most of the feathers studied are estimated to have color and brightness contrasts similar to values previously found for ripe fruit. On the other hand, for dichromat mammalian predators, visual contrasts for these feathers were only weakly detectable and often below detection thresholds for typical viewing distances. We also show that for dichromat mammal vision models, the peacock's train has below-detection threshold color and brightness contrasts and visual textures that match various foliage backgrounds. These findings are consistent with many feathers of similar hue to those studied here being inconspicuous, and in some cases potentially cryptic, in the eyes of common mammalian predators of adult birds. Given that birds perform many conspicuous motions and behaviors, this study suggests that mammalian predators are more likely to use other sensory modalities (e.g., motion detection, hearing, and olfaction), rather than color vision, to detect avian prey. This suggests new directions for future behavioral studies and emphasizes the importance of understanding the influence of the sensory ecology of predators in the evolution of animal coloration.

analysis, decision to publish, or preparation of the manuscript.

Competing interests: The authors have declared that no competing interests exist.

Introduction

Ever since Darwin, colorful feathers have been assumed to present salient visual signals readily detectable by their natural predators [1,2]. For this reason, sexually-selected ornaments like the iridescent eyespot feathers of the Indian peacock (*Pavo cristatus*) (Fig 1A) have been proposed to incur a cost due to increased predation [2–4]. As Zahavi argued in his paper introducing the handicap principle: "The more brilliant the plumes, the more conspicuous the male to predators" [5]. Evidence for such opposing selection pressures has been found in ornamented guppies preyed upon by fish [6]. On the contrary, susceptibility to cat predation was not found to correlate significantly with sexual dichromatism in birds [7], and a recent experimental study found that conspicuous plumage does not enhance predation by avian predators ([8] and references therein). Conspicuously-colored plumage also has been proposed to function as warning coloration for aposematism [9,10]. However, while these hypotheses are predicated on the predator being able to detect prey visual signals [11], no studies have tested whether

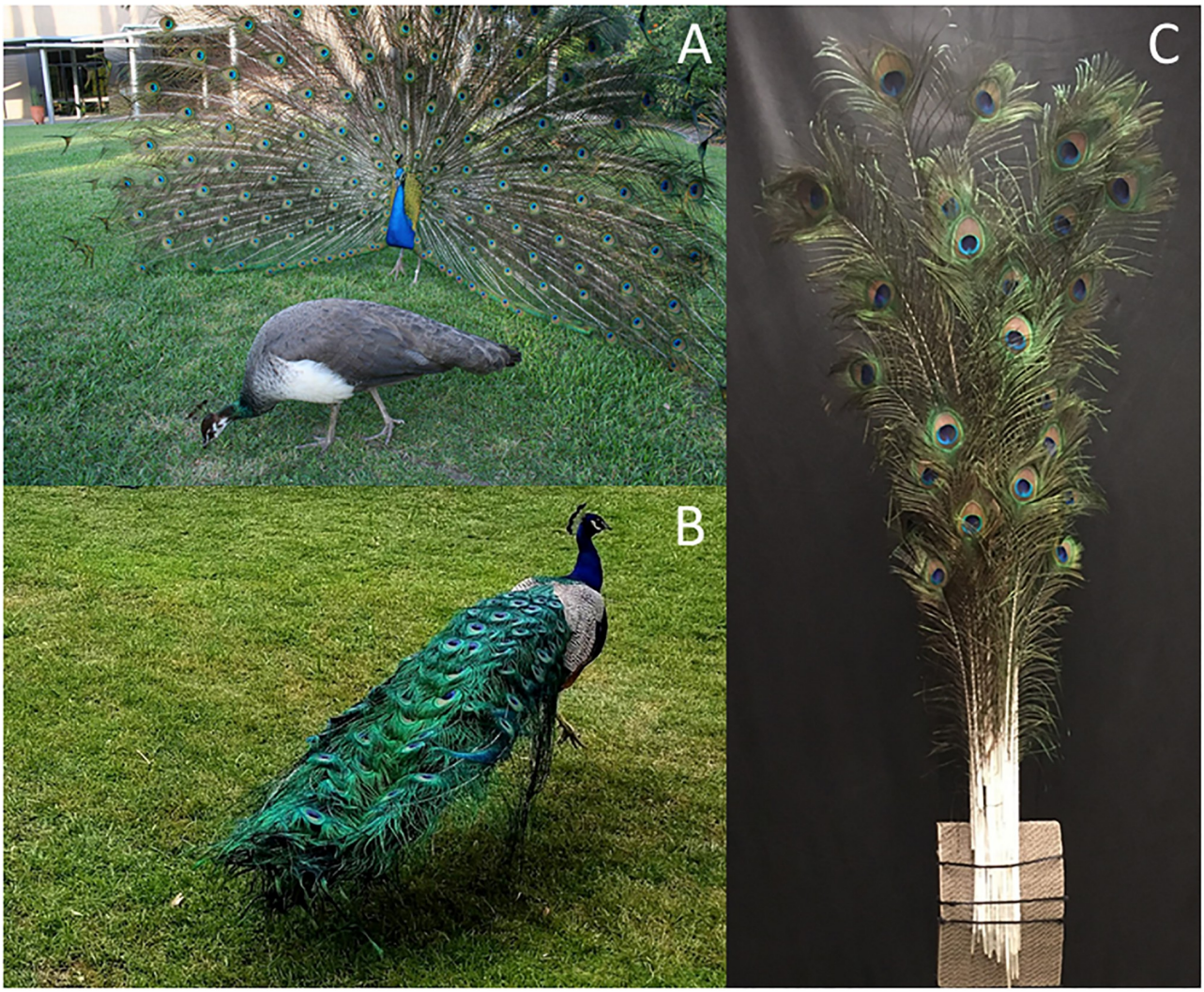

Fig 1. Peacocks and the model peacock train. A) An Indian peacock displaying his erect train to a peahen (female) in the foreground and B) another individual holding his train folded while walking. C) Model peacock train assembled from a collection of eyespot feathers used to evaluate the appearance of the train viewed against vegetation.

https://doi.org/10.1371/journal.pone.0210924.g001

this is true for the mammalian predators that prey on many birds. For example, the primary predators of adult peafowl are carnivorans (felids and canids, S1 Appendix), and cats are a major threat to bird populations world-wide [12]. These predators all have dichromatic visual systems; i.e., they have only two types of cone visual receptors with distinct spectral sensitivities, not the four characteristic of most birds or the three found in most humans [13]. Because dichromatic mammals lack red-green color discrimination, they are unlikely to detect many of the chromatic visual cues evident to birds and humans [13–15]. Studies of visual ecology have considered how prey appear to various types of predators (birds, insects and fish) for many types of prey, including insects and birds [16,17], fish [18], cuttlefish [19], crustaceans [20], primates [21] and lizards [11]. Two previous studies also have studied the iridescence reflectance spectra of peacock eyespots and how they are perceived by peahens (females) [22,23]. So far, no studies have compared how visual signals from peacocks and other birds appear in the vision of their mammalian predators.

During courtship displays, male Indian peafowl ("peacocks") attract mates by spreading, erecting and vibrating their fan-like train ornament (Fig 1A), causing it to shimmer iridescently and emit mechanical sound [24–26]. Several lines of evidence indicate that these feathers are assessed during mate choice: train-rattling performance by peacocks is obligatory for mating success [24], eye-tracking experiments have shown that train-rattling displays are effective at attracting and holding the peahen's gaze [27], and eyespot iridescence has been shown to account for approximately half of variation in male mating success [22,23,28]. Because peacocks spend the majority of their time in activities other than courtship displays even during the breeding season [24,29], any test of visual saliency must also consider the appearance of the folded train. Furthermore, because the peacock's head, neck and breast are covered by iridescent blue contour feathers [30], the visual cues generated by this body plumage are also relevant for salience to potential mates and predators.

Here, we use multispectral imaging to estimate how detectable peacock feathers are to conspecifics and dichromatic mammalian predators, as measured by color, brightness, and texture contrast relative to green background vegetation, following similar studies of prey that model camouflage against predators with a variety of visual systems [31]. We also use reflectance spectroscopy to compare the spectral reflectances of the various feather and foliage samples with each other, and with the known sensitivities of each viewing animal's photoreceptors. Our goal was to test the assumption that colorful feathers that are highly conspicuous to conspecific birds are also readily detectable by these predators. To determine how generalizable our results were to other hues of colorful plumage, we also measured reflectance spectra and multispectral images of red and yellow parrot feathers. We then used psychophysical vision models to estimate whether conspecifics and dichromatic mammalian predators can readily detect the color and brightness contrasts between feathers and green vegetation. Our analysis modeled the appearance of feathers at various distances to determine when each observing species could distinguish color patches relative to the surrounding environment. We also reviewed the literature to determine the light niches and sensory modalities used by mammals that prey on peafowl and other birds, and to understand whether an enhanced risk of predation has been documented for peacocks relative to other prey.

In addition to color cues, visual salience depends on the presence of pattern features that are perceptually discriminable from the background. To compute whether predators might detect the peacock's train using such visual texture cues, we analyzed images of live peacocks and of the model train relative to that of background vegetation using two pattern analysis methods motivated by visual processing in vertebrates [32]. Granularity analysis is a spatial filtering method that determines the contributions to image contrast of features with different sizes; this image processing technique has been used to compare pattern textures in studies of

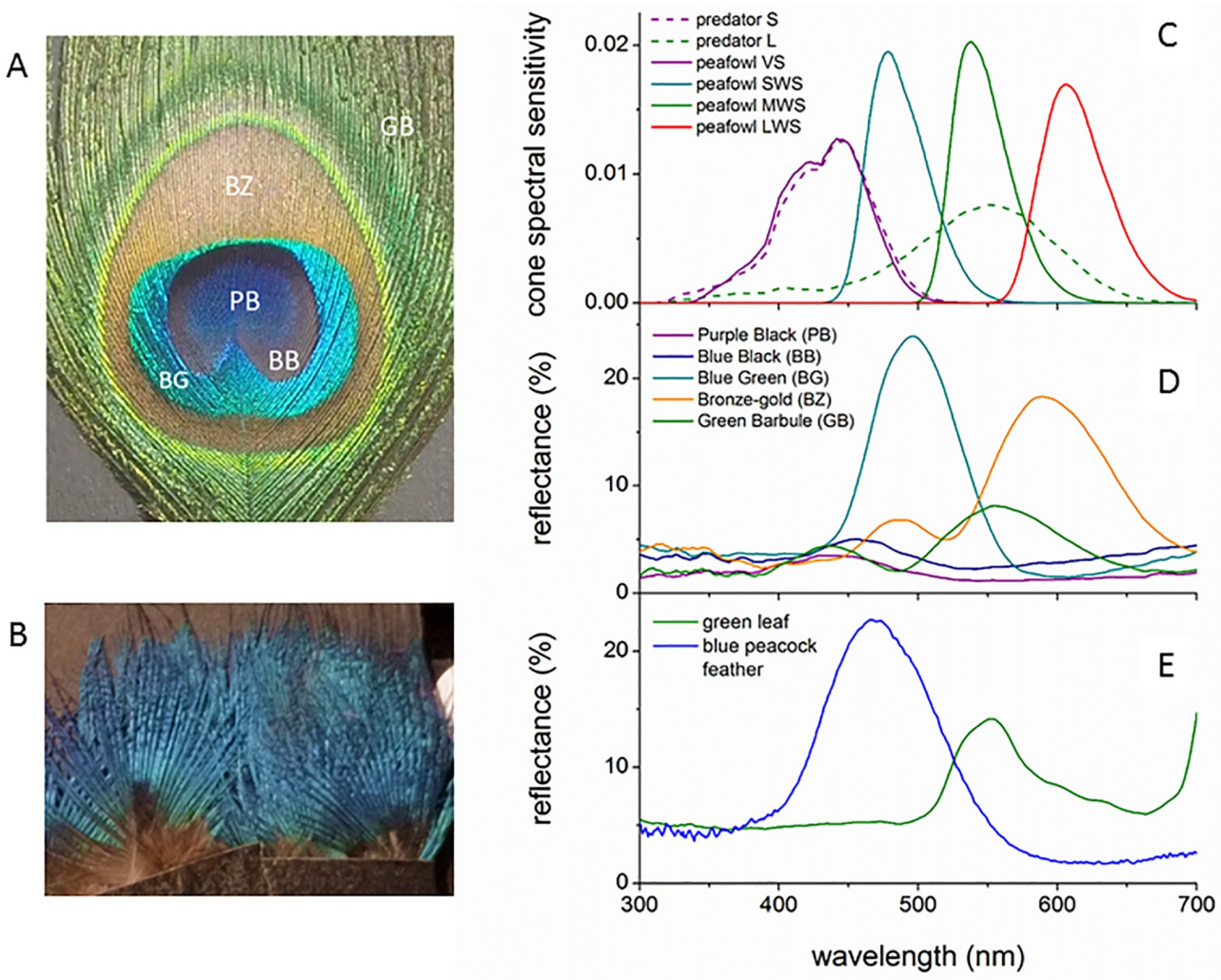

Fig 2. Peafowl feathers, cone sensitivity spectra and reflectance spectra for feathers and green vegetation. (A) An Indian peacock eyespot feather showing the color patch names used in the analysis. (B) Peacock blue breast plumage. (C) Comparison of the cone photoreceptor spectral sensitivities for the Indian peafowl and ferret, which has dichromatic color vision very similar to that of cats and dogs. All spectra are multiplied by the D65 illuminance spectrum used to model sunlight and normalized to unit area. Reflectance spectra of (D) peacock feather eyespots and (E) peacock iridescent blue body plumage and the green saucer magnolia (*Magnolia x soulangeana*) leaf used as a background for the feather sample images.

https://doi.org/10.1371/journal.pone.0210924.g002

cephalopod, avian egg, fish and shore crab camouflage, as well as humans searching for objects against various backgrounds [20,32–35]. A second method, edge detection, provides a complementary measure of texture complexity by using image processing to detect sharp gradients in intensity [36].

Materials and methods

Feather samples

Five Indian peafowl eyespot (Fig 2A), three blue peacock contour breast feathers (Fig 2B), four scarlet macaw (*Ara macao*) wing feathers (two red and six yellow patches total) (Fig 3A), two Amazon parrot (*Amazonica ochrocephala panamensis*) wing feathers (two red and two yellow patches total) (Fig 3B), and four red African grey parrot (*Psittacus erithacus*) tail feathers (Fig 3C) were obtained from Moonlight Feather (Ventura, CA USA) and Siskiyou Aviary (Ashland,

OR USA). Because the psittacofulvin pigments in parrot feathers have reflectance spectra with similar spectral features and reflectances as found for red and yellow carotenoid pigments [37–39], our results should be representative of red and yellow feathers in general. An earlier study of variation in color measurements for feathers [40] showed that three measurements per patch on one individual per species is sufficient for quantifying the colorspace coordinates of a feather color patch to within 5% of the mean as needed for our visual signal analysis. For mounting, eyespot feathers were cut off below the outermost colored ring at the proximal end. All feather types were mounted on black matte art quality paper with a magnetic backing that adhered to the tilt stages used for spectroscopy and multispectral imaging. Feather samples were stored without compression in sealed boxes in acid-free envelopes at 75% relative humidity and ambient temperature (22 ± 2 deg C). The different peacock eyespot color patches (colored rings and central disk) are referred to using the names and two letter abbreviations indicated in Fig 2A.

In addition to measuring the individual peacock feathers described above, we also created a model peacock train using an array of 28 peacock eyespot feathers (Fig 1C) arranged to match the geometry of eyespots in actual peacock trains [41]; this was used to simulate the appearance of the train during display (when the train is erect) or during walking, perching or standing (when the train is held horizontally; see Fig 1B). In their native range in India and Pakistan, peafowl are reported to live in a variety of habitats, including open moist and dry-deciduous forest, scrub jungle, and adjacent grasslands, and their breeding season is reported to coincide with the start of the rainy season [42], after which eyespot feathers are shed by molting [43,44]. Green leaves have a generic reflection spectrum due to their dominant pigment, chlorophyll, as determined for a variety of environments [45–47] including deciduous forests and other native vegetation in India [48,49]. To simulate the native habitat of peafowl during the day, we selected background vegetation using as reference images a variety of photographs of peafowl in India, Pakistan and Sri Lanka from the Macauley Library at the Cornell Lab of Ornithology and the Internet Bird Collection (details in S2 Appendix). The variety of background foliage selected from trees, brush and grasses from the midatlantic region of the USA (40.0093˚ N, 75.3057˚ W) (S3 Appendix) were selected to approximate the color, luminance and texture of many of the green plants found in the native environments of peafowl and many other bird species.

Vision models

The Indian peafowl's visual system has four classes of color-sensitive (chromatic) single cone cells: violet (VS), short (SWS), medium (MWS) and long (LWS) wavelength-sensitive cones, and one type of double cone that is sensitive to brightness (luminance) [50]. In order to illustrate their spectral responses under natural illumination, Fig 2C shows the peafowl cone's spectral sensitivities $S_r(\lambda)$ for the r^{th} photoreceptor class (including ocular media and oil droplet transmission) multiplied by the CIE D65 irradiance spectrum, $I(\lambda)$, and normalized to unit area; we used this standard illuminant because of its close match the solar irradiance spectrum for the elevation angles found for actual peacock displays [24,51]. To model the tetrachromatic UVS (ultraviolet-sensitive) vision of parrots we used blue tit (*Cyanistes caeruleus*) cone spectral sensitivities [52,53], which has peak spectral sensitivities that agree to $< 2\%$ with those of budgerigars (*Melopsittacus undulatus*), a type of parrot [54] (Fig 3D).

The visual systems of dichromatic mammalian predators have been studied for a variety of genera, and found to include S (blue- to near-UV-sensitive) [55] and L (green-sensitive) cone populations in all carnivorans studied to date, including felids [56] and canids [57]. Behavioral studies have confirmed that domestic cats [58] and dogs [59,60] have dichromatic color vision.

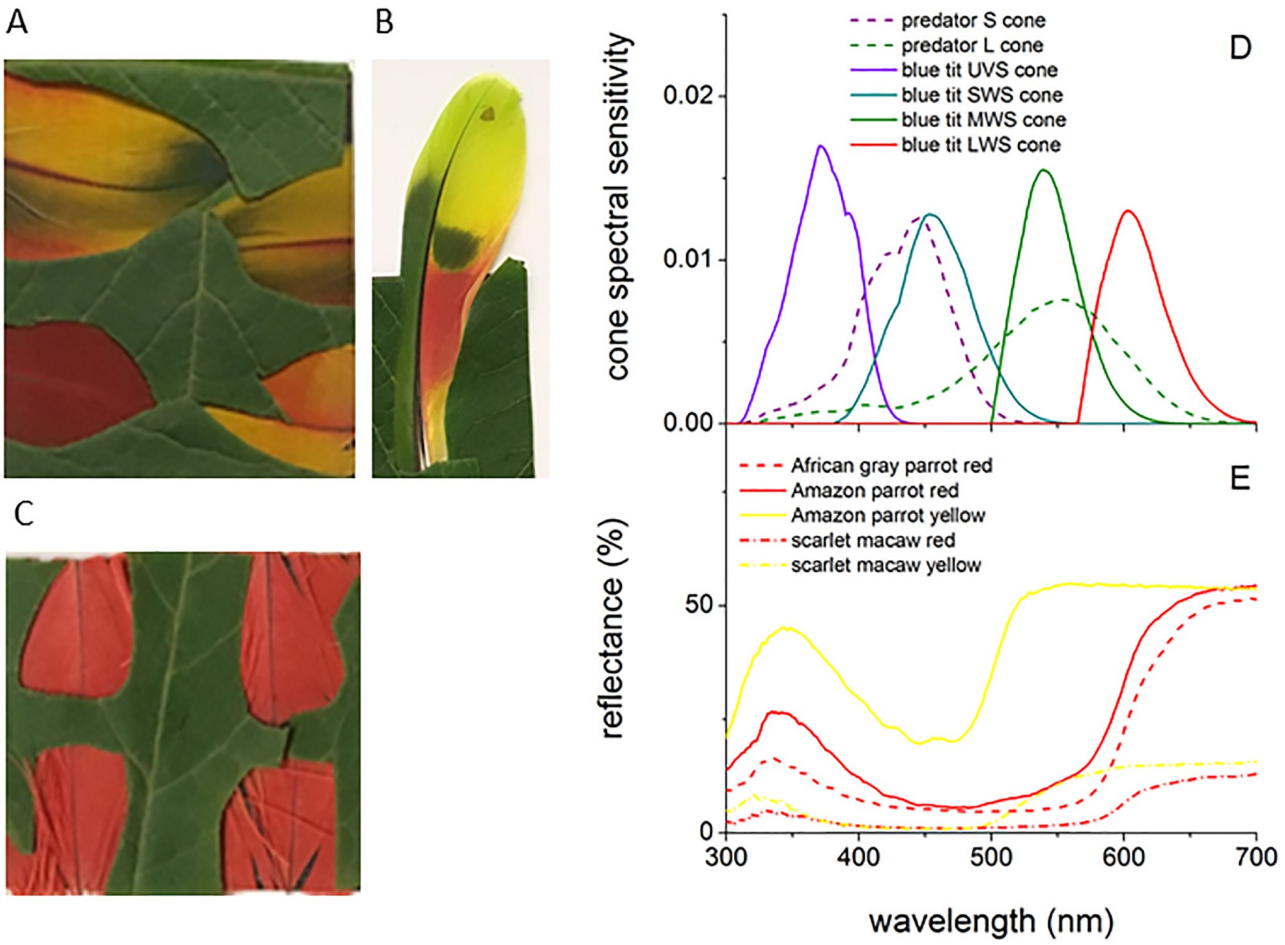

Fig 3. Parrot feather images, cone sensitivity spectra and feather reflectance spectra. (A) Scarlet macaw, (B) Amazon parrot and (C) African grey parrot feather samples. (D) Comparison of the cone photoreceptor spectral sensitivities for the blue tit, which has tetrachromatic ultraviolet sensitive (UVS) color vision similar to that of parrots, and the ferret, which has dichromatic color vision similar to that of cats and dogs. All spectra are multiplied by the D65 illuminance spectrum used to model sunlight and normalized to unit area. (E) Reflectance spectra of the parrot feather red and yellow patches studied here.

https://doi.org/10.1371/journal.pone.0210924.g003

Brightness signals in dichromatic mammals are assumed to be due to only the L cones [61]. We used ferret (*Mustela putorius*) cone spectra [53] to model dichromat vision because ferret spectral peaks agree closely with those of cats, dogs and foxes (i.e., $\leq$ 4.4% for S and $\leq$ 1.4% for L cones) [56,57,62] (Fig 2C).

Like many other primarily diurnal birds, peafowl are active throughout the day, with a peak in their foraging and display activities in the morning (post dawn) and late afternoon. Ecological studies have used camera trapping and radiotelemetry tracking to measure diel activity patterns of wild cats and dogs in Southeast Asia and the neotropics. The results show that many of these potential predators of peafowl and other wild birds are active and hunt during the daylight hours as well as crepuscular and nocturnal conditions, and that many are primarily diurnal [63–70]. Animal-borne video methods have shown that free-ranging feral domestic cats, a major predation threat to wild birds, often hunt during daylight hours as well [71]. Wild felids are reported to hunt primarily using vision [72]. Dholes (*Cuon alpinus*), a wild canid reported to prey on peafowl, are reported to have good vision and olfaction, and to locate prey primarily by sight rather than by scent [73]. Domestic dogs and cats, as well as coyotes (*Canis latrans*),

another wild canid, have been shown to use both vision and olfaction in a variety of contexts (e.g., [60,74,75] and references therein), including to locate prey [76]. Thus, it is relevant to consider whether these predators use color signals and photopic (high luminance) vision to locate prey. Under low light conditions, chromatic signals will be weak and visual signals will be dominated by luminance contrast via rod photoreceptors, which have a spectral sensitivity similar to that of the luminance channel for these mammals [77,78]. In addition, a predator's visual acuity and ability to distinguish contrast is greatly diminished under low light conditions [79–82]. Therefore, we modeled visual perception of visual signals by these predators for photopic conditions, to give the best case scenario for detection.

Reflectance spectroscopy

We measured reflectance spectra using a model USB2000+ spectrometer and OceanView software (Ocean Optics, Largo FL, USA) over the wavelength range 300–850 nm, using 100 ms integration time, 3 pixel boxcar averaging (corresponding to the optical resolution of 6.5 pixels = 2.06 nm FWHM), and averaging over 5 samples. All spectra were recorded in a dark room. Samples were illuminated by an Ocean Optics PX-2 Pulsed Xenon Light source triggered at 200 Hz using square wave pulses from a model 330120A function generator (Agilent Technologies, Wilmington, DE, USA); the source was turned on and allowed to warm up and stabilize for 15 minutes before data collection. Light for illumination and detection was carried in P400-1-UV-VIS optical fibers transparent to 200 nm (Ocean Optics). We used two PTFE white standards with flat 99.0% reflectance over 300–700 nm: a Spectralon USRS-99-010-EPV (Labsphere, North Sutton, NH USA) and a model SM05CP2C (Thorlabs). White standard and dark currents were measured every fifteen minutes. For each feather and each measurement geometry, raw reflectance spectral data were recorded for each feather color patch sample radiance, AR, white standard radiance, AR_r and dark current, D. The reflectance spectrum, $R(\lambda) = \frac{AR-D}{AR_r-D}$, was smoothed over a wavelength interval of 20 nm using Savitzky-Golay smoothing in Origin; this reduced high frequency noise but did not change reproducible features of the spectra peak shapes.

Transmission spectra for the filters used in multispectral imaging were measured by recording the spectrum of light reflected from the white standard with and without the filter inserted into the light path with its face at normal incidence to the incident light. Reflectance values for color and gray standards were measured using a RPH-SMA reflectance probe stand (Thorlabs, Newton NJ USA) with the illuminating light at 45 deg to normal incidence and detected at normal incidence. The reflectance goniometer for feather measurements used (S2 Fig) was adapted from previously published designs [83,84] but with an additional angular degree of freedom to allow measurement of the bidirectional reflectance distribution function, in which the angle of observation and illumination are not confined to the specular reflection geometry [85]. Both the illumination and detection optical pathways were focused using a 74-UV lens (Ocean Optics) to a 2 mm diameter spot at about 5 cm from the output surface of the lens. The feather samples were realigned every time the angle of illumination and/or detection was adjusted to ensure both beams focused on the same region of the feather. To assess reproducibility of spectra for the same color patch on each feather, we measured each set of spectra three times for each sample after dismounting and remounting each sample.

Multispectral imaging

Multispectral imaging allows the measurement of color and luminance signals from across an entire feather, or array of feathers, under natural environmental lighting conditions (including the effect of reflected light from green background vegetation); it also allows modeling of the

effects of blurring due to visual acuity limitations [86]. The methods used here involve recording two images of the same sample photographed through different filters, including reflection standards to allow measurements of absolute reflectances. The different combinations of filters and camera color channels then are analyzed using visual models for the viewing animal of interest. Multispectral images were recorded using a GoPro Hero 4 Silver Edition camcorder (GoPro Inc, San Mateo, CA USA) modified for full spectral imaging by replacing its original lens and infrared (IR) filter with a quartz lens transparent to < 300 nm [87,88]. Because the spectral response of this camera's IMX117 Exmor-R CMOS sensor (Sony Corp., Tokyo, Japan) is sensitive throughout the visible and near-UV, these cameras have been used in multispectral imaging [89,90] (S1 Fig). Multispectral photographs were recorded at 3000 × 2250 pixel resolution and the GoPro settings medium field of view, Protune CAM-RAW mode (for no white balance compensation), flat color, low sharpness, ISO 400, exposure -2, night mode (to enable shutter speed control), auto shutter and spot meter on. Each sample was photographed twice for each geometry and illumination condition to give two multispectral images: 1) a UV image using an Andrea-UV filter (< 1% transmission for > 400 nm; UVIROptics, Eugene, Oregon USA; 2) a visible RGB (red, green, blue) image using two UV-IR cut filters to pass 400–700 nm light (Hoya Corp., Tokyo Japan). Filter transmission spectra were measured using the methods described in "Reflectance Spectroscopy" (S1 Fig). The camera's large depth-of-field eliminated the need for refocusing between visible and UV images. To maintain constant camera alignment between photographs, we mounted the camera rigidly using optical mounts (Thorlabs, Newton NJ, USA) and attached filters using quick-release Xume magnetic adapters (Panalpina Inc., Port Reading, NJ, USA); all images were taken using a remote trigger. Each feather image included a model Micro FSS08 8-step grayscale diffuse reflectance standard (Avian Technologies, New London, NH USA) mounted level with the sample plane for calibrating absolute reflectance [53]. Images of the model train included a larger 6-step grayscale and color checker chart (DGK Color Tools WDKK Waterproof, Digital Image Flow, Boston MA USA). Reflectance spectra for each grayscale in each filter and camera color channel combination were measured using the methods described in "Reflectance Spectroscopy". Each image also included an object of known size for spatial calibration.

All samples were mounted on a tripod for imaging (S2 Fig). Three sets of multispectral images each were obtained with the model train held erect and held horizontal viewed from the side. Peacock eyespots were oriented with their rachis vertical to simulate their average orientation in the erect train during courtship displays and the model train was oriented in a variety of directions to simulate the variation in appearance of the iridescent train eyespot feathers during courtship display, standing and walking. The camera was mounted on a second tripod a distance 20.0 ± 1.0 cm from feather samples and 1.70 to 2.00 ± 0.05 m from the model train. For feather samples, the camera was oriented to record images at normal observation angle ($\theta = 0 \pm 2$ deg) with respect to the feather sample plane (Fig 4). The size of feather sample images was 55 mm x 67 mm, corresponding to 7.3 pixel/mm. Images were captured during June-July 2018 in the Haverford College Arboretum (latitude, longitude: 40.0093˚ N, 75.3057˚ W) for 24.2 ± 0.2 deg C and 55.5 ± 1.5% relative humidity. All feather samples were illuminated by direct sunlight with an azimuthal angle $\Psi = 45 \pm 3$ deg clockwise from the camera's optical axis and at solar elevation angles $\Phi = 30 \pm 3$ deg, corresponding to an angle $\alpha = 52 \pm 3$ deg between the observation and illumination directions (Fig 4). These illumination and observation angles agree with those measured for female peafowl observing courtship displays in the morning and late afternoon [24]; they also agree with the angle found to enhance reflectance contrast between the two largest color patches in the peacock's eyespot [23]. In general, these solar angles hold for the morning times when most birds are most active [91–93]. Optimal color contrasts for non-iridescent feathers have been found to correspond to the range of

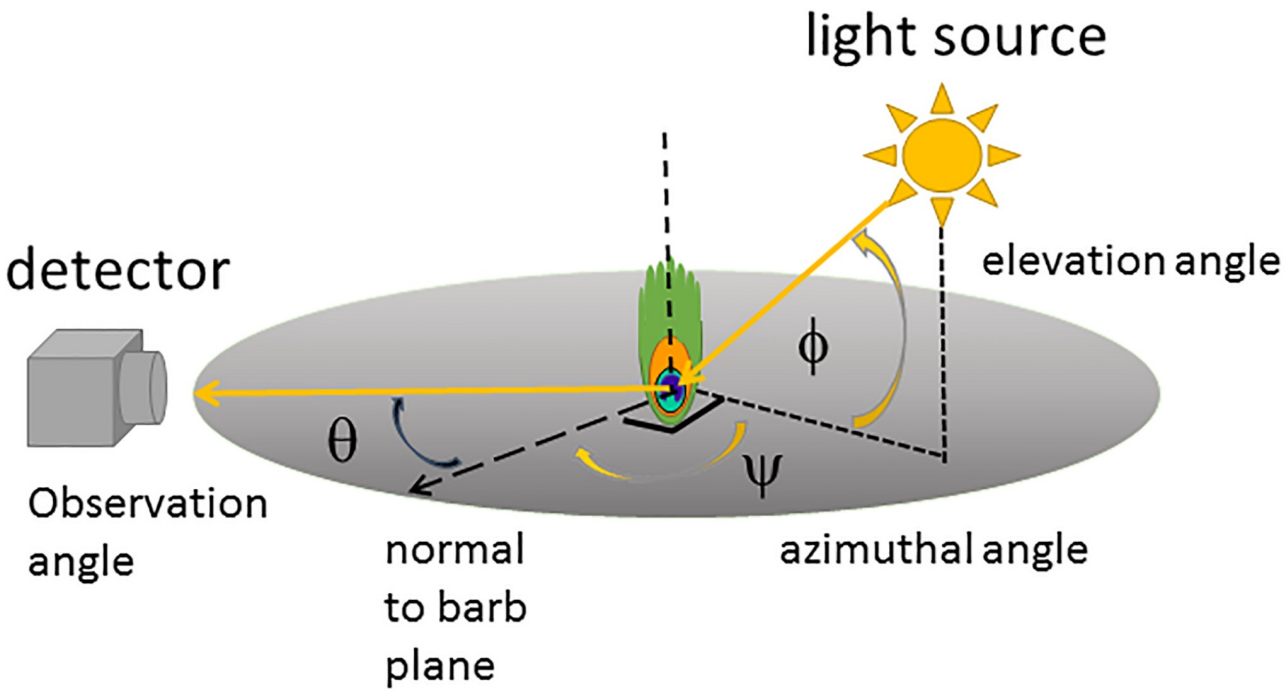

Fig 4. Multispectral imaging geometry showing the angles of observation and illumination.

https://doi.org/10.1371/journal.pone.0210924.g004

observation-illumination angles α used in this study [94]; this is relevant because pigment-based colors can appear in combination with structural coloration [38]. In addition, for this observation geometry, the bird's body subtends the greatest visual angle. The peacock eyespot feather samples were surrounded by additional loose green barbs to simulate their setting in the actual train, while the parrot feather samples were surrounded by saucer magnolia (*Magnolia x soulangeana*) leaves picked $\leq$ 1 hour before image capture. We also imaged a variety of green leaves for comparison (S3 Fig). Black velvet fabric was mounted behind the feather samples to limit backscattered light and a lens hood was used to reduce lens flare. The model peacock train was photographed against a variety of foliage backgrounds for solar elevation angle between 37 to 55 deg.

Multispectral images were first processed using custom scripts written in MATLAB v15a with the Machine Vision, Signal Processing and Fitting toolboxes (MathWorks, Natick MA USA); all code is available on figshare at https://figshare.com/s/688fb19dad98b6273324. Images stored as jpeg files were calibrated and corrected for lens distortions using the MATLAB Camera Calibration application, and then corrected for perspective distortions using MATLAB's *fitgeotrans* and *imwarp* commands. Images captured using the UV and visible filters were checked for alignment by hand and then converted into linearized and normalized measures of reflectance, as explained under "Quantitative visual signal analysis" below.

To account for distance-dependent blurring due to each viewing species' visual acuity [95,96], multispectral images with linearized intensities were spatially filtered before analysis to model the effect of viewing distance on contrasts between feathers and background foliage, and its effect on contrasts within the patterned eyespot feathers (See details in S4 Appendix). While peahens view peacock courtship displays at nearby distances $\geq$ 1 to 2 m [24], we also modeled a variety of greater viewing distances (2, 4, 8 and 16 m). Color patches were defined by hand in the original images and used for each modeled distance for uniformity. Following

[97], to ensure that intensity samples were independent, we sampled each image using a square grid with spacing equal to a visual acuity disk, after spatial filtering and before color and brightness analysis. To model the effect of spatial filtering on the peacock's blue head, neck and breast plumage, we used an image with green foliage background with an approximately peacock-shaped cutout of the blue plumage superimposed; spatial filtering was performed using peacock body dimensions [98] to define the composite image's effective spatial scale.

Quantitative visual signal analysis

The color and brightness contrast perceived by an animal depends on the reflectance of adjacent patches as well as the sensitivities of the animal's photoreceptor cone types. Quantitative models for computing these contrasts have been developed and well-validated (see review in [99]). We computed the color contrast, ΔS_c, between color patches in the feathers and background vegetation in our multispectral images using the receptor noise limited color opponent model, which has been shown to predict behavioral thresholds for visual signals in birds, humans and insects [100]. All calculations were performed using a custom MATLAB script, which was tested by verifying that it computed the same values as the multispectral analysis software package MICA version 1.22 [53]. First, intensity values, V, from each multispectral image were corresponded to the actual reflected irradiance, R, for this camera by an S-log transformation:

$$R(V) = Ae^{-\frac{V}{T_o}} + C. \quad (1)$$

The parameters A, T_o and C were obtained from nonlinear least squares fits in MATLAB (adjusted-$R^2 \geq 0.997$) of the measured V and R values for each pixel in each RGB channel of the image for the 8-step grayscale. The resulting fits then were used to convert measured intensity values for each p^{th} color patch into linearized and normalized reflected intensities (range [0,1]) for each combination of filter and RGB image channel. To compute the color and brightness contrasts, these intensities were converted into the cone quantum catch values, Q_{pr}, for each of the viewer's r^{th} cone photoreceptors:

$$Q_{pr} = \int I(\lambda)R_p(\lambda)S_r(\lambda)d\lambda / \int I(\lambda)S_r(\lambda)d\lambda, \quad (2)$$

where $I(\lambda)$ is the illumination spectrum, $S_r(\lambda)$ is the r^{th} cone receptor's normalized spectral sensitivity and $R_p(\lambda)$ is the p^{th} patch's reflectance spectrum. Because birds and mammals are known to achieve color constancy under a wide variety of illumination conditions [101,102], this equation also incorporates the von Kries transformation, a mechanism for maintaining color constancy [103]. To accomplish this conversion, we used MICA to compute the parameters of a polynomial cone mapping between the UV filter blue channel and the visible filter RGB channels of the multispectral images recorded by our filter-camera system and the corresponding cone quantum catches, Q_{pr} [53,86]. This software finds the optimal mapping using our measured filter transmission and camera RGB spectral response curves with either the dichromatic ferret or tetrachromatic peafowl cone spectral sensitivities, the CIE D65 illumination spectrum and a large database of natural spectra. The net effect is to combine all measured values of linearized and normalized reflectance to compute the quantum catch, Q_{pr}, of each r^{th} cone (r = S or L for dichromats and r = VS, SWS, MWS, or LWS for tetrachromats) for the p^{th} sample color patch. Using a linear 2-way interaction cone mapping model, we obtained a near perfect fit for each visual system: ferret ($R^2 \geq 0.999$), peafowl ($R^2 \geq 0.996$) and blue tit (≥ 0.990 UVS cone, ≥ 0.998 all other cones).

The resulting cone quantum catch values, Q_{pr}, can be used to compute normalized color space coordinates, for the pth color patch: $q_p = \frac{Q_{pr}}{\sum_r Q_{pr}}$. For tetrachromats, the receptor index r = VS or UVS, SWS, MWS, LWS and q_p = (v,s,m,l), while for dichromats r = S, L and q_p = (sw,lw). After normalization, this corresponds to a three-dimensional tetrachromat color space for birds and a one-dimensional colorspace for dichromats, here chosen to rely on sw. Following [104], to validate the results of our multispectral imaging code, we compared dichromat color space sw coordinates computed by both MICA and our MATLAB code (sw_M) from our multispectral images with those computed directly from reflectance spectra (sw_R) for six color chart squares. Use of the camera and UV/visible filter cone mapping model was validated for multispectral image analysis by the goodness of the linear fit, zero intercept and unit slope, between the two sets of color space measures gave $sw_M = (0.018 \pm 0.031) + (1.00 \pm 0.07) \times sw_R$ + (adjusted-$R^2 = 0.993$) (S1 Fig).

To compute color contrasts, ΔS_c, we first computed the rth cone's log-linear quantum catch (Weber-Fechner), log Q_{rp}, for each pth patch. This was used to compute the difference in rth cone response for the pqth patch pair, $\Delta_{rpq} = \log Q_{rp} - \log Q_{rq}$. The color contrast then is computed from differences between opponent cone pairs weighted by receptor noise. Dichromats have only S/L receptor opponency, so for them, $\Delta S_C = |\Delta_{Lpq} - \Delta_{Spq}| / \sqrt{e_L^2 + e_S^2}$ [100]. The corresponding equation for color contrast in tetrachromats is more complicated because all six possible combinations of the four single cones pairs should be considered [105]:

$$\Delta S_C^2 = \frac{\begin{pmatrix} (e_S e_{VS})^2(\Delta_L - \Delta_M)^2 + ((e_M e_{VS})^2(\Delta_L - \Delta_S)^2) + \\ (e_S e_M)^2(\Delta_L - \Delta_{VS})^2 + (e_S e_L)^2(\Delta_M - \Delta_{VS})^2 + \\ (e_S e_M)^2(\Delta_L - \Delta_{VS})^2 + (e_L e_M)^2(\Delta_{VS} - \Delta_S)^2 \end{pmatrix}}{(e_S e_M e_L)^2 + (e_{VS} e_M e_L)^2 + (e_{VS} e_S e_L)^2 + (e_{VS} e_S e_M)^2} \quad (3)$$

For bright illumination levels, receptor noise is assumed to be a constant determined only by the Weber fraction, w_f and the relative population density, g_r, for each rth cone class [99]: $e_r = w_f / \sqrt{g_r}$. For peafowl, we used the value for chromatic Weber fractions of $w_f = 0.06$ for L cones for domestic chickens based on color discrimination [106]. Receptor noise values for the other single cone classes were estimated using mean peafowl relative population densities g_r = (0.477,0.892, 1.047, 1) for (VS, SWS, MWS, LWS) [107], yielding e_r = (0.087, 0.064, 0.06, 0.06). For parrots, we used g_r = 0.25:0.33:1.05:1 and $w_f = 0.105$ found for spectral sensitivity in budgerigars [54], corresponding to e_r = (0.210, 0.182, 0.102, 0.105). Because color discrimination has not been measured for non-human mammals [81], following [108] we used $w_f = 0.22$ found for brightness discrimination in domestic dogs (range 0.22–0.27) [109]. The relative cone population fractional densities measured for domestic cats [110] give a mean g_r(S,L) = (0.12,1); similar ratios have been reported for various wild felids [111] and domestic dogs [112]. This gives the estimated predator receptor noise for color discrimination as (e_S, e_L) = (0.64, 0.22).

The brightness contrast, ΔS_L, between each pqth pair of color patches was computed from the quantum catches, Q_{Lp} for the pth color patch for the spectral response for the luminance channel (double cones for birds and L cones for dichromat predators) using $\Delta S_L = (\log Q_{Lp} - \log Q_{Lq})/w_f$, where w_f is the Weber fraction for brightness discrimination. For birds, we used $w_f = 0.18$ measured for double cones in budgerigars [113]; for comparison, lower values 0.10 have been found for pigeons [114] and higher values ≥ 0.24 for chicks of the domestic chicken [115]. For predators, we used $w_f = 0.22$ for brightness discrimination in domestic dogs as

explained above; for comparison, $w_f = 0.10$ in humans [81,116] and $w_f = 0.42–0.45$ for the horse, the only other terrestrial mammal for which data exist [81,117].

Color and brightness contrasts are interpreted in units of just noticeable distances (JND), with JND = 1 corresponding to the threshold for two patches to be discriminable under ideal illumination and viewing conditions when suitable data exist for the visual system being modeled [100,106]. Behavioral studies have shown that birds detect colorful fruit at a rate that correlates with increasing color (but not brightness) contrast for values >> 1 JND [118], while in lizards, the probability of discriminating a color from its background was found to be < 20% at 1 JND and to scale approximately linearly over the range $1 \leq \text{JND} \leq 12$ [119]. Behavioral tests in zebra finches have found that color contrast detection thresholds range from JND = 1 to 2.5 to 3.2, depending on background color [120]. Following [121], we therefore assume that the contrast detection threshold is approximately JND = 1 and we define contrasts in the range $1 < \text{JND} \leq 3$ as weakly detectable.

Simulated avian and mammalian predator images

Using MATLAB, we also generated "false color" images intended to provide human viewers with a simulation of the colors, intensity and contrasts perceived by a different visual system. The intensity in each color channel on a false color image was calculated from the square-root transformed quantum catch measured for the appropriate cone species; this intensity mapping corresponds approximately to the human perception of brightness [122]. Following [53], we represented the tetrachromatic vision of birds using two images: 1) an RGB image created from the transformed LWS, MWS and SWS cone catch data, respectively; 2) a fourth grayscale image created from the transformed VS or UVS cone catch. After [19], we represented the two color channels of dichromatic mammals using a single RGB image by setting the blue channel equal to the transformed S cone quantum catch and the yellow (red + green) channel equal to the transformed L cone quantum catch. To accompany the texture analysis, we also generated an additional luminance-only grayscale image using the transformed luminance cone quantum catch.

To compensate for the greatly reduced color and brightness contrast discrimination value for the dichromatic predators relative to humans, we reduced the brightness and color contrasts of dichromat images as follows. Dichromat false color images generated as described above were first converted into CIE $L^*a^*b^*$ colorspace [122]. We then adjusted the brightness contrast for both the luminance and yellow-blue images. To do so, we rescaled the L^* (luminance) channel to a new value L^*_{fc} so as to maintain the same mean intensity over the entire image while reducing the contrast. This was accomplished using the formula: $L^*_{fc} = w_{Lh} / w_{Ld} \times (L^* - L^*_m) + L^*_m$, where L^*_m = the mean luminance in the image, and the brightness contrast Weber fractions were $w_{Lh} = 0.14$ for humans and $w_{Ld} = 0.22$ for dogs [81]. For the yellow-blue images only, we also rescaled the color contrast by multiplying the b (blue-yellow opponency) channel in the $L^*a^*b^*$ image by w_{Ch} / w_{Cd}, where $w_{Ch} = 0.06$, the color contrast Weber thresholds for humans [106], and $w_{Cd} = 0.22$, the value for dogs: $b_{fc} = b \times w_{Ch} / w_{Cd}$. (The red-green opponency channel, a, was zero everywhere in these false color images since the red and green channels are set equal.) The resulting images reflected the reduced contrast perceived by a dichromatic mammal with the given Weber fraction.

Pattern analysis

To model the perception of visual texture of the peacock's train viewed against foliage, we also performed granularity pattern analysis on the model peacock train photographs, using MATLAB code adapted from [34] and MICA's granularity texture analysis package [53]. In

granularity analysis, an image based on the luminance channel is filtered using an FFT bandpass filter centered at a series of spatial frequencies (granularity bands). For each bandpass-filtered image, the "pattern energy" (a measure of information at each spatial scale) is computed as the standard deviation of its pixel intensity values. The "granularity spectrum" then is defined as pattern energy vs granularity band. Granularity analysis was performed on the model peacock train images processed for the dichromatic predator luminance channel as explained above. Granularity spectra were computed for polygonal regions of interest (ROI) encompassing the entire model train and each type of surrounding vegetation (i.e., tall grass, brush or trees). To compensate for the effect of ROI shape and background, we used the following method adapted from MICA. For each ROI, we first computed a masked image in which all regions outside the ROI were replaced by a black background. Next, we created a mean masked image in which the region inside the ROI in the masked image was replaced by the mean intensity within the ROI. Identical granularity calculations were performed on both images and their difference was used to create a shape-independent granularity spectrum.

We also computed granularity spectra and summary statistics for comparing textures of the model train and its background [32,34]. The summary statistics comprised: total energy (the energy summed across all filter bands, which increases as pattern contrast increases), peak filter size (the granularity band at peak energy; larger peak filter size corresponds to smaller most prevalent feature size), and proportion energy (the maximum energy divided by the total energy, a measure of how much of the spectral energy lies at the most prevalent feature size; this decreases with increasing pattern scale diversity). Granularity spectra were plotted as "normalized energy" (pattern energy divided by total energy) vs granularity band to give a measure of how pattern information is distributed across spatial scales. Images with a uniform distribution of pattern scales have correspondingly uniform granularity spectra, while images dominated by a single feature scale should have strongly peaked spectra.

Edge detection of the luminance channel image provides an alternative measure of pattern complexity. The basic idea is that image processing algorithms can find edges in good agreement with human perception by calculating the local maxima of image intensity gradients [122]. We used the Canny edge filter in MATLAB to find edges using sigma = 3 and threshold = 0.15 to 0.20 (relative to maximum luminance image intensity set to 1) [80,123]. Model train images were first log transformed and then processed using contrast-limited adaptive histogram equalization [124] (*adapthisteq* in MATLAB) to detect texture edges in regions of widely differing illumination. The edge fraction (percentage of edge pixels in each ROI) was then used to compare the model train with various types of vegetation in the background [36]; higher edge fractions indicate a more complex pattern with more spatial features.

To provide a source of images for pattern analysis that correspond directly to foliage in the peacock's native habitat, we searched for photographs of Indian peacocks in the Macaulay Library at the Cornell Lab of Ornithology and the Internet Bird Collection [125] (S2 Appendix) that showed peacocks with full trains in a variety of orientations with eyespots visible against native green vegetation. Photographs were used only if they did not appear to have been selectively contrast or color enhanced, and if images of both birds and vegetation were unblurred and of sufficient resolution. A total of 14 images satisfied these conditions. While we could not use these photographs for multispectral analysis because they lack the required calibrations, we could determine a good approximate to the luminance using the green image channel because the green channels of digital cameras have spectral sensitivities that approximate that of L cones (e.g., Fig 2D and [86]). Consequently, granularity and edge detection analyses were performed on grayscale images based on the green channel of each photograph. Because photographs were taken from a variety of distances from the peacocks, we normalized

the peak filter size (most prominent spatial feature scale) for each photograph by the peak filter size for the peacock's train to allow comparison between photographs.

Statistical analysis

Our analysis of color and brightness contrasts followed the two-step process recommended in [126]. First, to determine whether the mean color and brightness contrasts between each patch pair had a statistically significant difference given their variances, we used PERMANOVA modified for non-normal, heterogeneous data [127] implemented in the software package FATHOM [128] using 1000 bootstrap samples. Note that is it possible for this difference to be statistically significant, but to have a value too small for it to be perceptually distinguishable. We therefore determined the effect size (how perceptually distinct each color patch pair) as follows. We first drew with replacement 1000 bootstrapped sample pairs using the MATLAB command *datasample*, and computed the mean ΔS_C and ΔS_L for this bootstrap resample. These mean contrasts were averaged over all images to get the mean and s.e.m. for each color patch pair for each sample; the grand mean and s.e.m. then was computed by averaging over all replicates for each feather type. Grand means and s.e.m. for the texture summary statistics were calculated from the mean of each statistic taken over all model train data for the train, grass, brush, and tree foliage. All results are reported as grand mean [95% CI = 2 s.e.m].

Data accessibility

All data and software required in order to replicate all of our results are archived either in the supplemental materials or at https://figshare.com/s/688fb19dad98b6273324.

Results

Literature review of predation on peafowl

A review of the literature (S1 Appendix) did not uncover evidence that peacocks with full trains experience an enhanced predation risk, but rather supports the idea that wild adult peafowl are preyed on infrequently by mammals in their native habitats and that the highest risk of predation is primarily during the first year [129]. (Note that peafowl have different plumage in their first year and that males do not develop the fully grown train and eyespots (the focus of this study) until their third or fourth year.) For example, one study found that wild peafowl are preyed on far less by leopards than expected given that they were the most abundant prey species in the region studied [130], another that dholes and tigers preyed on peafowl less than expected based on their density [131] and a third that peafowl were a "significantly avoided prey species" in a review of prey selection by tigers [132]. In addition to these results for wild peafowl in native habitats, one survey of a feral peafowl population [133] found that, among adult peacocks with full-grown trains, the males that were preyed on tended to have relatively small trains and lower mating success. Another study of feral peafowl found that adult peacocks preyed upon by domestic dogs and red foxes (*Vulpes vulpes*) had half the predation risk as adult female peafowl and the same number of eyespots and mating success and a slightly longer train (5.2 ± 2.4%, based on 3 predated males) as surviving adult males [134]. Adult peacocks are reported to have several effective anti-predator strategies, including running [135], flight [136], fighting with their sharp spurs [28], hiding in dense thickets [29,129,135], roosting in high trees chosen for their protection against predators at dusk [129,137], and using group vigilance along with alarm calling [138]. Consistent with this, three studies have shown that the peacock's train does not significantly hinder locomotor performance during flight or walking; indeed, peacocks walking on a treadmill were efficient compared to other avian bipeds for

which data exist and had a reduced metabolic cost during the breeding season when their trains were fully grown [136,139,140].

Reflectance spectroscopy

Reflectance spectra for peacock eyespot feather color patches (Fig 2D) and peacock iridescent blue plumage (Fig 2E) had spectral peaks consistent across repeated measured to 4 to 16 nm (95% CI) and exhibited similar spectral peaks and overall shape to those measured for zero elevation angle [22,23,30]. A comparison of cone spectral sensitivity data (Fig 2C) with these reflectance spectra show that the peacock SWS cone is well matched to reflectance from its iridescent peacock blue plumage. While the spectral peaks for the bronze (BZ), blue-green (BG) and outer loose green (GB) barbs agree well with its SWS, MWS and LWS cone spectral ranges, all three also coincide with the same L cone sensitivity for the predator. Both the predator and peafowl VS cone spectral sensitivities also overlap with the reflectance spectrum from the eyespot's central BB and PB dark violet patches. However, reflectance from these features is weak compared to the other color patches, all of which also reflect weakly in the UV. Fig 2E shows the reflectance spectrum of a representative green leaf, illustrating how its peak at approximately 550 nm and its overall spectra resemble that of the peacock's loose green barbs; similar spectra for green background foliage have been reported in (Cazetta, Schaefer, and Galetti 2009; Loyau et al. 2007).

Reflectance spectra for parrot feathers (Fig 3E) agreed with previously published values [141], confirming a good spectral match between yellow and red feather reflectance with MWS and LWS avian cone sensitivities. The predator L cone sensitivity spans a spectral range corresponding to longer wavelength reflection from both yellow and red pigments (Fig 3D). Both the yellow and red patches also have reflectance peaks in the UV with a better overlap with bird UVS cone sensitivity than that of VS cones.

A comparison of the peak spectral sensitivities of S and L cones for canids, domestic cats and ferrets with those for the four single cone populations of 21 bird species from 8 different orders [142] (Fig 5) illustrates that predator S cones have a peak response similar to that of bird VS, but not UVS, cones. The predator S peak values lie between most peaks of the avian UVS/VS and SWS cone populations, whereas predator M peak values lie between avian MWS and LWS peak values.

Color and brightness contrast analysis

False color images and analyses using the receptor noise model of visual discrimination are shown in Figs 6–9; all data and PERMANOVA pseudo-F and P values are reported in S1–S4 Datasets.

False color images for various simulated viewing distances are displayed for peacock eyespot feathers in Fig 6A and visual signals are plotted vs distance in Fig 6B–6E. In peafowl vision, all pairs of adjacent color patches in the peacock's eyespot give large, statistically significant color contrasts > 3 JND for all distances. The greatest color contrasts were between the blue-green patch and surrounding rings and between the two central pupil-like patches; for some distances ≤ 8 m these same pairs of color patches also had statistically significant brightness contrasts in the 1–3 JND low detectability range. By contrast, in dichromat vision none of the eyespot patch pairs had color contrasts above 1 JND, and only the three innermost pairs of eyespot patches had brightness contrasts that were in the weakly detectable 1–3 JND range.

For peafowl vision, at all distances the model peacock train had statistically significant color and brightness contrasts that were > 3 JND for brush and trees, but not grass (Fig 7; additional false color images in S4 Fig). In dichromat predator vision, all color contrasts for the model

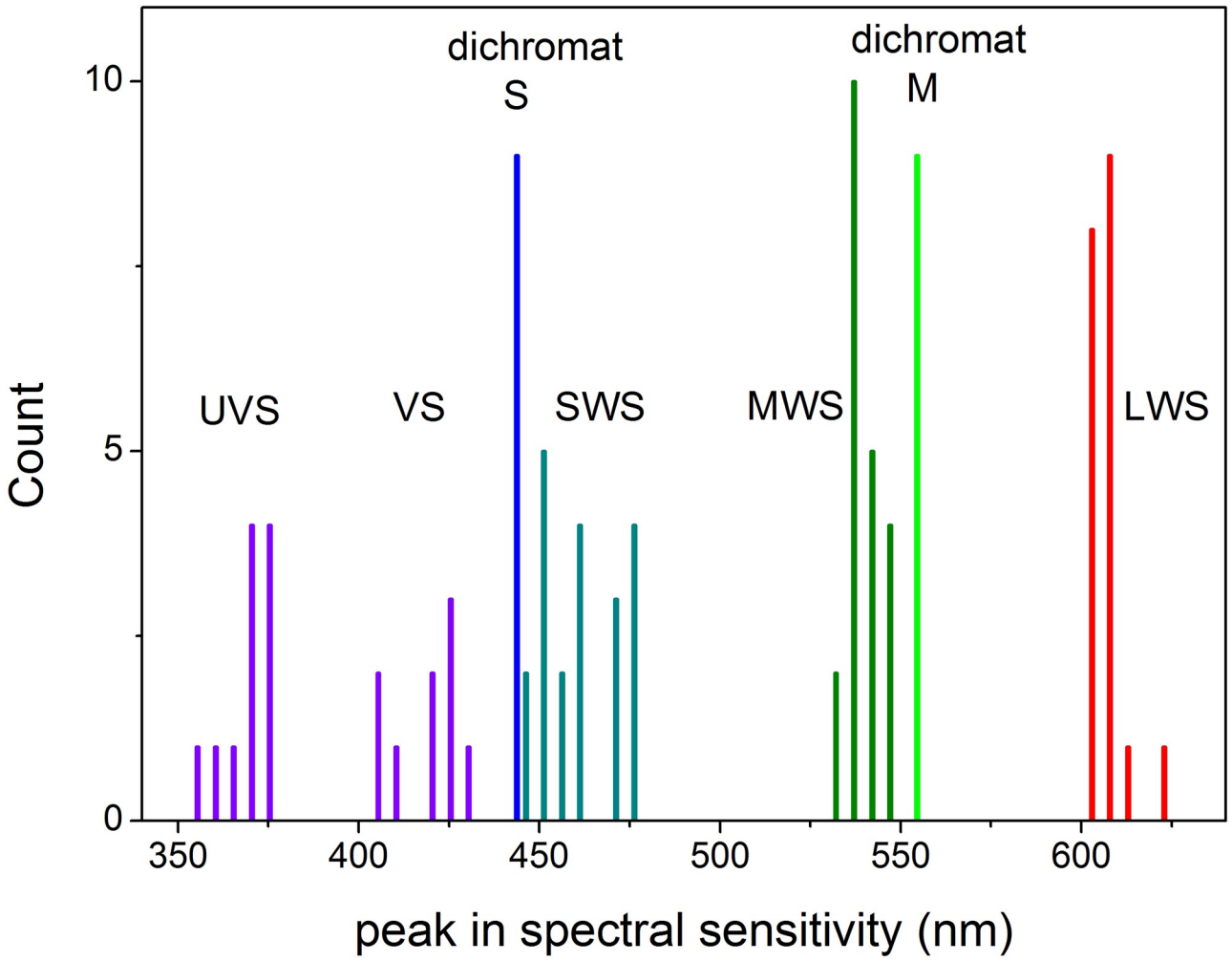

Fig 5. Comparison of peak spectral responses of predator and bird cones. Peak single cone spectral sensitivities for ferret S and L cones (Douglas & Jeffery, 2014) and for bird VS/UVS, SWS,MWS and LWS cones from Fig 5B in (Hart & Hunt, 2007) for 21 species of birds from 9 orders.

https://doi.org/10.1371/journal.pone.0210924.g005

train were < 1 JND and brightness contrasts were in the weakly detectable 1–3 JND range. Peacock blue plumage was found to be perceptually detectable by conspecifics at all distances and to lie in the weakly detectable 1–3 JND range for dichromat vision (Fig 8). The false color images of peacock feathers (Figs 6, 7 and 8, S4 Fig) demonstrate how color signals relative to background vegetation are diminished when the single dichromat L cone replaces the separate SWS/MWS/LWS cones for birds, especially at larger distances.

Red and yellow parrot feather color patches exhibited large, statistically significant contrasts in avian UVS vision in general, with color contrasts > 3 JND for ≤ 8 m and brightness contrasts > 1 JND for most samples (Fig 9). By contrast, for dichromat vision, none of the red parrot patches and the African grey parrot and scarlet macaw yellow patches had color contrasts > 1 JND, and the Amazon parrot feather yellow patches just exceeded 1 JND for ≤ 4 m. For distances ≤ 8 m, red parrot feather patches had brightness contrasts in the weakly detectable 1–3 JND range for ≤ 8 m and yellow patches had mean values in the range 2.4–6.7 JND.

We also measured the contrasts between leaves from the background leaf used (saucer magnolia) and seven other plant species with different shades of green. For dichromat mammal

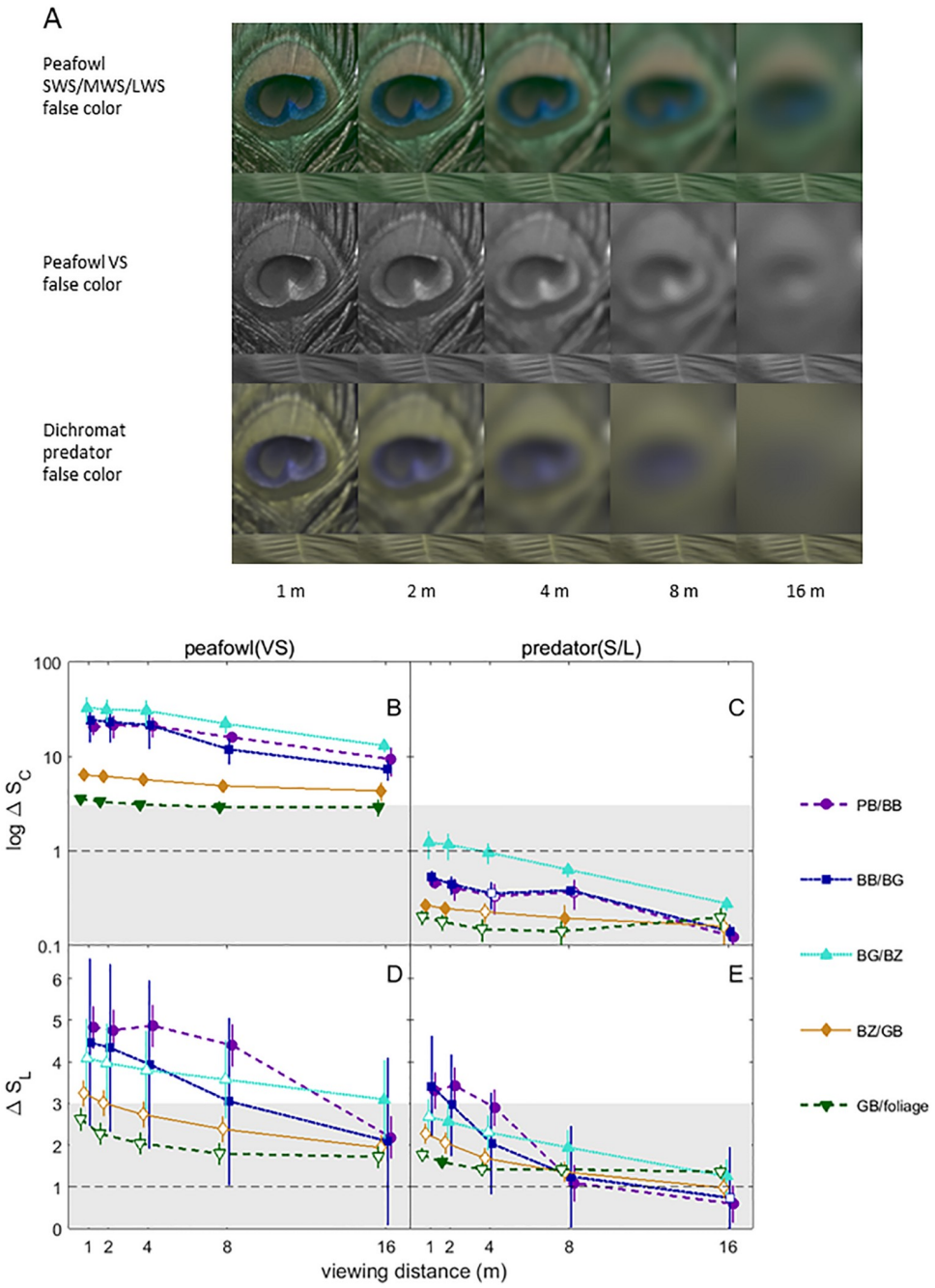

Fig 6. False color images and color and brightness contrast analysis of peacock eyespot feathers. (A) False color images modelling peafowl and dichromatic mammalian predator vision of peafowl eyespot and green leaf (inset at bottom of eyespot image) for different viewing distances. Note that the false color images should be considered as a relative guide and not an absolute indication of the detectability of contrasts because humans have better contrast thresholds by a factor of 3.7 for color and 2 for brightness compared to dichromatic mammals. (B)-(E) Estimated color (delta S_C) and brightness (delta S_L) contrasts for adjacent color patches on the peacock eyespots and green vegetation, over a range of viewing distances. All data are shown as grand means with 95% CI error bars. Contrasts corresponding to the same distance have been displaced by horizontal jitter to avoid overlap. Data above the 1 JND line are above the expected threshold for discrimination and contrasts within the grey shaded regions are at most weakly detectable. Closed symbols indicate contrasts that are statistically significant in each organism's colorspace (i.e., PERMANOVA $P < 0.05$); note that contrasts that are not statistically significant (closed symbols) due to their large, overlapping variances in the corresponding colorspace may still have mean values greater than the detection threshold.

https://doi.org/10.1371/journal.pone.0210924.g006

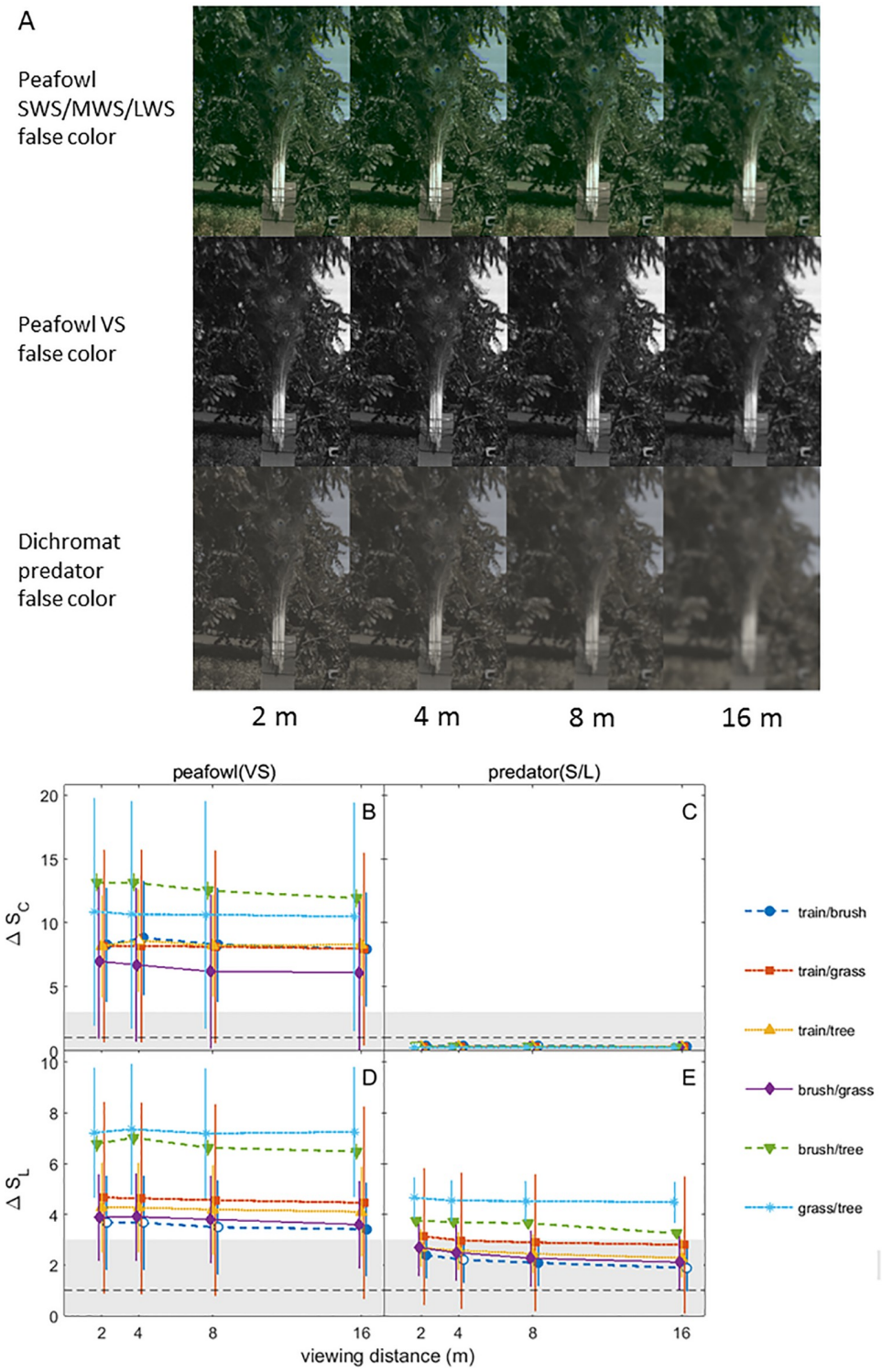

Fig 7. False color images and color and brightness contrast analysis of the peacock model train photographed against various types of vegetation backgrounds. (A) False color images in peafowl and dichromatic mammalian predator vision of peafowl model train for different viewing distances. (B)-(E) Color and luminance contrasts for the model train and features of vegetation, over a range of viewing distances. All data are shown as grand means with 95% CI error bars. See Fig 6 caption for further details.

https://doi.org/10.1371/journal.pone.0210924.g007

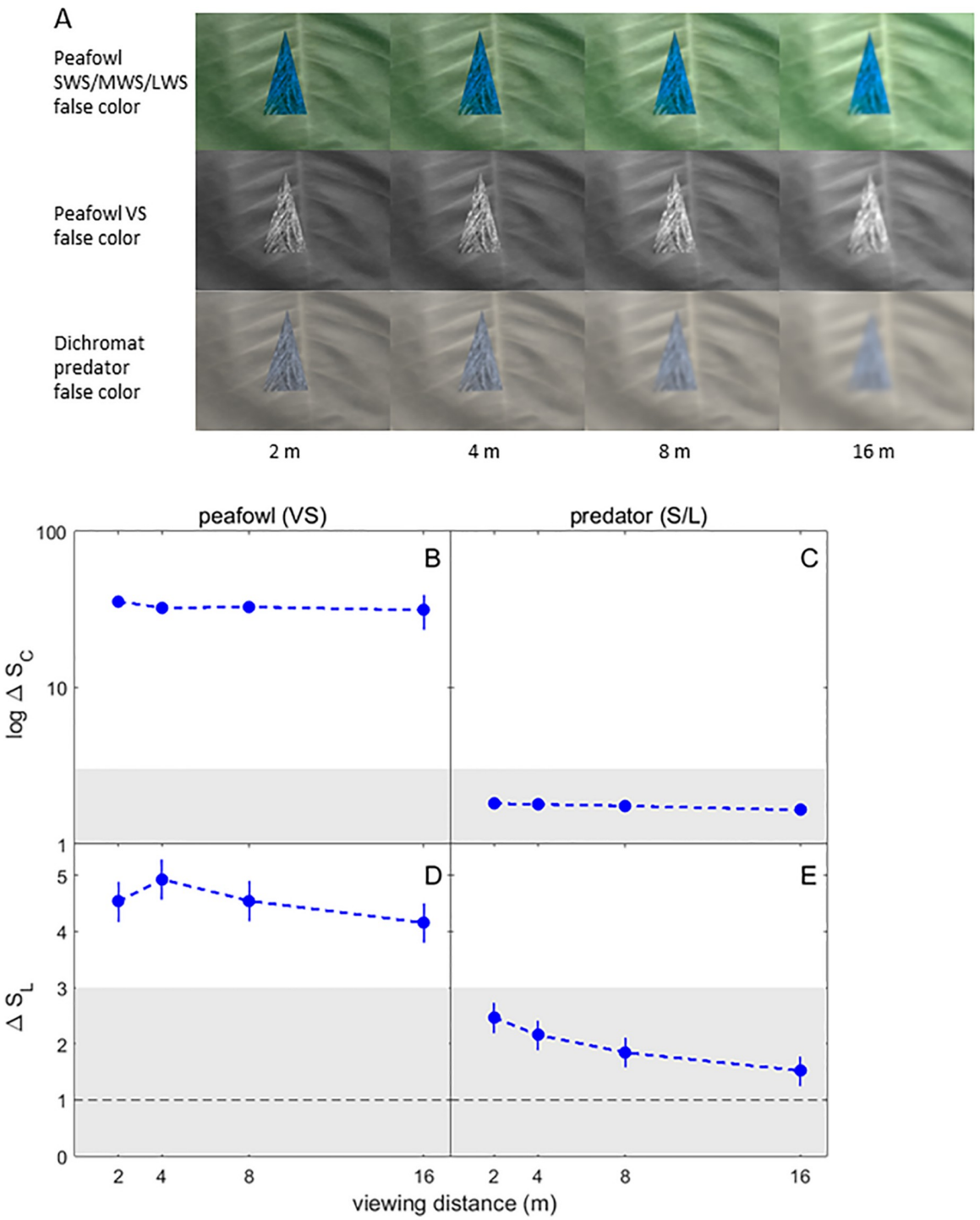

Fig 8. False color images and color and brightness contrast analysis of peacock blue neck feathers used to model the body's appearance against green foliage. (A) False color images in peafowl and dichromatic mammalian predator vision of peacock blue breast plumage vs green foliage for different viewing distances. (B)-(E) Color and luminance contrasts for the blue plumage relative to green vegetation, over a range of viewing distances. See Fig 6 caption for further details.

https://doi.org/10.1371/journal.pone.0210924.g008

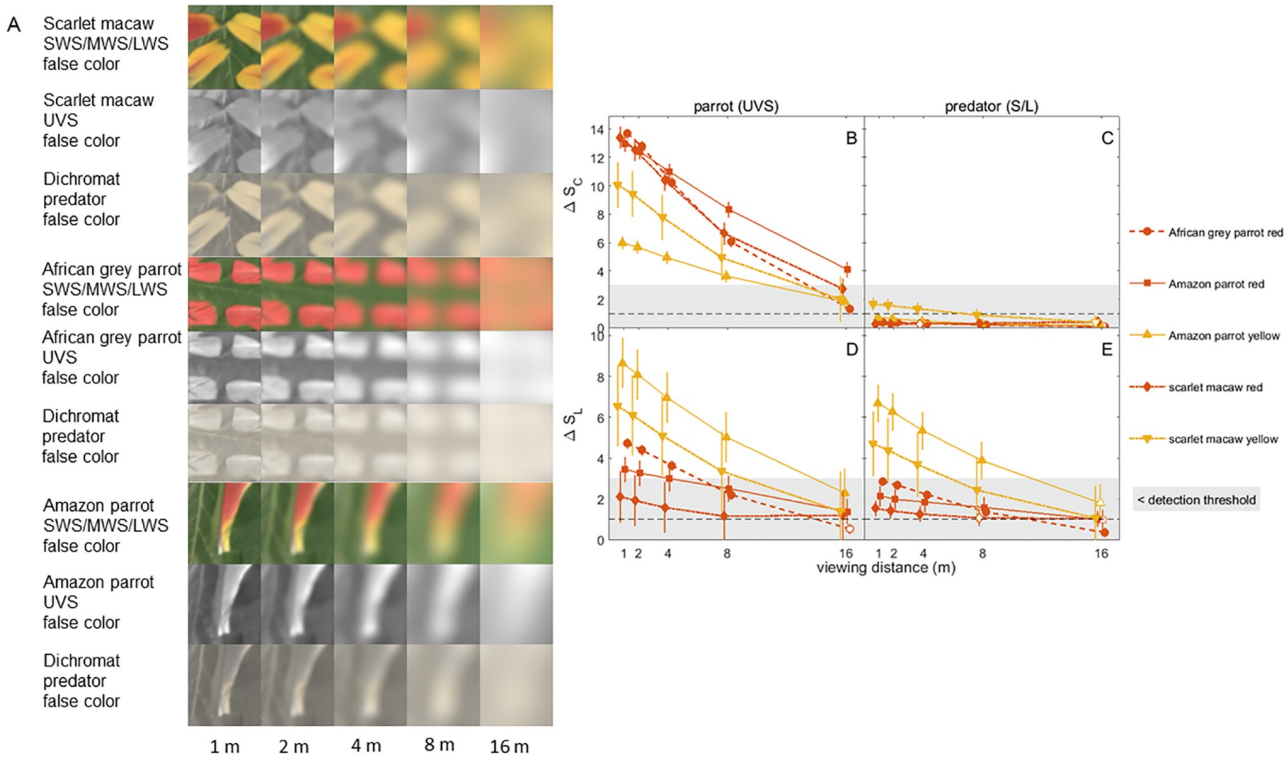

Fig 9. False color images and color and brightness contrast analysis of parrot feathers. (A) False color images in parrot ultraviolet sensitive (UVS) and dichromatic mammalian predator vision of scarlet macaw, African grey parrot and Amazon parrot red and yellow feathers vs green leaf for different viewing distances. (B)-(E) Color and luminance contrasts for parrot feather colors relative to green vegetation, over a range of viewing distances. See Fig 6 caption for further details.

https://doi.org/10.1371/journal.pone.0210924.g009

vision, the contrasts for these leaf pairs were $\Delta S_C = 0.55$ [0.42, 0.69] and $\Delta S_L = 2.53$ [2.01, 3.06] (mean [95% CI]). (S3 Fig). These values correspond to an additional source of uncertainty for the feather visual contrasts. These between-leaf color contrasts are too small to change the conclusions for the feather color contrasts discussed above. The values for brightness contrast suggest that the brightness contrasts for very dark or very light feathers viewed against very light or very dark green foliage, respectively, could correspond to the readily detectable range. The corresponding values for tetrachromatic bird vision ($\Delta S_C = 2.75$ [2.23, 3.28] and $\Delta S_L = 3.30$ [2.64, 3.97]) are also small compared to most of the corresponding feather-foliage JND values, consistent with birds being able to detect the high JND feather patches relative to leaves over many distances.

Pattern analysis

Fig 10 and S4 Fig show false color images and granularity spectra for the multispectral images of the model train and different types of background vegetation (tall grass, brush and trees) for the various viewing distances modeled (S5 Dataset). Table 1 gives summary statistics for the pattern analysis of online photographs and S6 Fig shows the corresponding granularity spectra. Because the spatial frequency of objects in an image as well as an animal's visual field depend on distance, we would expect objects with similar textures observed at different distances to have similarly-shaped spectra, but possibly different frequency peaks and widths. Granularity spectra for the model train (Fig 10B) indeed had the same shape as those for background vegetation in that each had a single broad peak for granularity band values > 3; similar

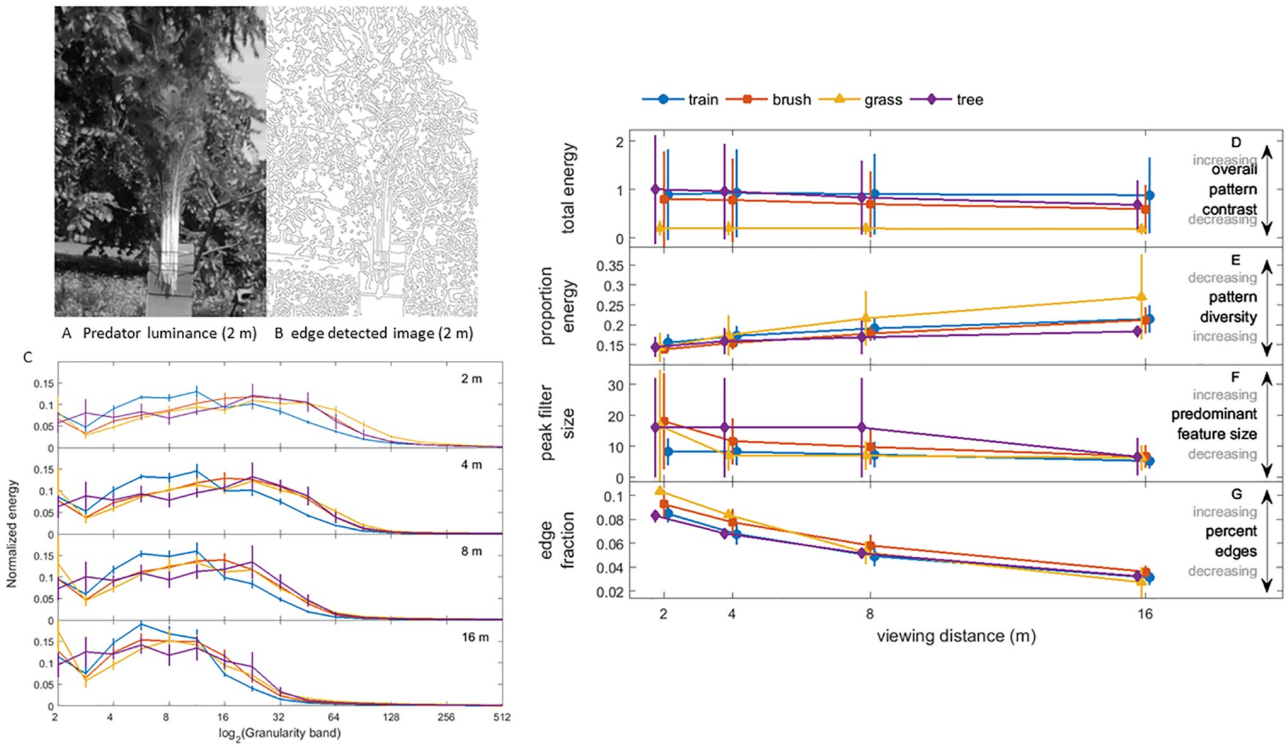

Fig 10. Texture analysis of the model peacock train photographed against various vegetation backgrounds. (A) Image based on dichromatic mammalian predator luminance channel and (B) result of edge detection on the luminance image. (C) Granularity spectrum for the model peacock train and three different regions of vegetation in the background vs viewing distance. (D) Total spectral energy summed over the granularity spectrum, which gives a measure of overall pattern contrast. (E) Proportional energy, a measure of how much the dominant feature size dominates and hence pattern diversity; (F) spatial frequency at peak spectral energy, which is inversely proportional to the predominant feature size; (G) edge fraction, the proportion of the image corresponding to edges. Data are grand means for all model train images and error bars show 95% CI.

https://doi.org/10.1371/journal.pone.0210924.g010

results were found for trains of live peacocks photographed against native habitats (S6 Fig). The peak spatial frequencies of each granularity spectrum moved to lower values as viewing distance increased, as expected from the blurring of fine scale features (Fig 10C). For all distances, the model train and background vegetation had values of proportion energy, peak frequency and total energy that agreed at the 95% CI, with the only exception that the proportion energy for distances > 4 m differed between the model train and trees (Fig 10D–10F). Similarly, the summary statistics for pattern analysis of photographs of the trains of live peacocks and native vegetation all agreed at the 95% CI level (Table 1). Collectively, these results demonstrate that the peacock's train is an excellent match for the predominant feature size distribution, overall contrast and pattern scale diversity of a variety of background vegetation. Moreover, visual examination of the edge detected images (Fig 10A, S5 Fig) supports the finding that the calculated edge fractions for the model train and trains of live peacocks and background foliage agreed at the 95% CI level at all distances (Fig 10G, Table 1).

Table 1. Texture analysis results for images from online sources (grand means [95% CI]).

	Total energy	Proportion energy	Peak filter (normalized)	edge fraction
train	0.47 [0.05, 0.88]	0.13 [0.12, 0.14]	1	0.036 [0.015, 0.056]
brush	0.65 [0.34, 0.96]	0.13 [0.12, 0.14]	2.0 [1.0, 3.0]	0.037 [0.014, 0.061]

https://doi.org/10.1371/journal.pone.0210924.t001

Discussion

The results of our study show that sexually-selected color signals readily detectable by conspecifics are not necessarily conspicuous to mammalian predators. Instead, for all distances considered, the color and brightness contrasts for all feather samples studied here relative to green foliage were much greater for birds than for dichromatic mammals. For all viewing distances modeled here, most feather samples had color contrasts in dichromatic predator vision that were perceptually indistinguishable from background vegetation; two exceptions were in the low detectable range: the peafowl's blue plumage (color contrast range [1.6, 1.8] JND) and the yellow scarlet macaw feather patches (color contrasts [1.6, 1.7] for $\leq$ 2 m). Unsurprisingly, the same feathers were highly conspicuous to conspecifics: their color contrasts were comparable to values found for avian visual modeling for fruit viewed against green foliage [118,143]. The brightness contrasts for these feathers vs background foliage in dichromatic predator vision were on the whole greater than the corresponding color signals, although only values for yellow exceeded the weakly detectable 1–3 JND range. This suggests that patterns with high brightness contrast, such as those created by white and dark melanin-pigmented plumage, might be more readily detectable by dichromat predators than color signals, and thus represent a greater detection risk [144]; such brightness-based visual signals also would presumably be more readily detectable for low light conditions. While the interpretation of supra-threshold color and brightness contrasts is still debated [145], our results show that such supranormal stimuli remain detectable by conspecifics and other birds even at large distances where carnivores cannot perceive them.

Peacock plumage in dichromatic predator vision

Focusing now on peacock eyespots, the large color contrasts for peafowl vision arise from spectral tuning between the reflectance spectra of each peacock eyespot color patch and peafowl single cone spectral sensitivities, similar to the agreement reported earlier between red and yellow pigment reflectance spectra and tetrachromatic UVS cone responses for parrot plumage and vision [141]. It is especially notable that the greatest color contrasts are due to the blue-green ring, since its iridescence has been found to correlate with peacock mating success [22,23], and its chromatic contrast was calculated to be the most salient signal in images of a displaying peacock [146].

When we computed measures for the model peacock train against a foliage background in dichromatic predator vision, the train feathers were found to have below detection threshold color contrasts and brightness contrasts in the low detectability 1–3 JND range, similar in magnitude to those for various types of green vegetation. Pattern analysis also indicated that peacock train feathers have similar textures to many types of vegetation in their native habitats. Taken together with the eyespot and textural analysis results, this indicates that dichromatic mammalian predators are likely unable to discriminate the peacock's train from green vegetation during foraging, although the eyespot's innermost features create low detectable brightness contrasts at nearby distances.

The peacock's blue plumage had large, detectable levels of color contrast at all distances for peafowl vision, though both color and brightness contrasts were in the low detectable range for dichromatic predator vision. Thus, the blue head, neck and breast contour feathers may represent a greater visual signal for distant conspecifics, as well as a greater predation risk, than the much larger train; however, all of these values are likely less conspicuous when forest shade diminishes their blue hue. Given that noniridescent blue feathers from other birds have been shown to have similar reflectance spectra to peafowl blue plumage, these results are likely generalizable to blue feathers from other species of birds [147].

In addition to color and pattern effects, salience can also be influenced by particular shapes. For example, some authors have speculated that the concentric shapes on the peacock's train plumage might be especially salient because of the resemblance to eyes [148]. Indeed, it has been shown that eyes and eye-like patterns are highly salient visual signals for birds, humans and domestic dogs [149–151]. However, our false color images show that peafowl eyespots do not always appear to have a central dark, circular pupil when viewed at typical display distances, either in peafowl or dichromatic mammalian predator visual models (Fig 11). Therefore, it is not obvious that peacock ocelli appear eye-like to nearby viewers. On the other hand, blurring at larger distances $\leq$ 8 m causes eyespots to appear to have pupil-like dark centers in both peafowl and dichromatic predator vision, indicating that they may indeed appear eyelike to predators when viewed at this intermediate range (Fig 11D–11F).

Taken as a whole, these results do not support the hypothesis that the peacock's eyespot feathers are highly conspicuous for all viewers. The measured color and brightness contrasts and pattern textures indicate that eyespot feathers could serve as disruptive camouflage [31] under some conditions (e.g., for peacocks viewed in their native scrub jungles) by breaking up the train's outline and making it more difficult to distinguish from surrounding foliage. Indeed, [152,153] noted that even to humans the peacock's train can be well camouflaged against foliage in its native habitats. This could be useful when wild peafowl roost in trees at night and when they spend the hottest hours of the day in dense thickets of brush [129,135,154]. Based on such reports, it has been suggested [155] that peafowl eyespots originated as a form of camouflage for their native dappled light environments. Note, however, that during much of the day, peafowl perform many actions (e.g., foraging, calling and displaying) in open spaces, and during these times other cues are likely to render them conspicuous to predators. Our results suggest that their colors are not likely to add appreciably to their predation risk during these times.

Motion cues during peafowl displays and other behaviors might enhance the detectability of their visual signals, although evidence is mixed whether motion increases or decreases visual contrast thresholds [156]. On the other hand, the motions of the flexible loose green barbs in the train might also simulate that of background brush and grasses, a visual illusion studied in insects, crabs, spiders and lizards but not yet in birds [157]. To elucidate the effect of motion on visual signals during displays, future video studies could utilize cameras adapted for multispectral imaging provided with a filter that transmits light from the near-UV to 700 nm, allowing modeling of dynamic visual signals in dichromat vision.

These conclusions are consistent with the lack of evidence in the literature that peacocks with trains experience a significant, let alone an enhanced, risk of predation compared to, e.g., either peacocks without trains or peahens. The available evidence thus indicates that any handicap suffered by adult peacocks is likely to be incurred by factors other than visual signals created by their eyespot train feathers. For example, peacocks spend a large percentage of their time maintaining their plumage [158] and displaying [24,29]. Thus, the elaborate courtship displays of peacocks may correspond to handicaps due to visual signals from their blue plumage, time lost from foraging for food due to plumage maintenance and courtship displays, the male's likely inattention to predators during displays, and the metabolic demands of the male's courtship displays [159].

Red and yellow pigmented plumage in dichromatic predator vision

Considering now red and yellow feathers, we note that red plumage is at best weakly detectable given its sub-threshold color contrasts and low brightness contrasts when viewed by dichromatic mammals against green foliage (although yellow parrot feathers have brightness

Fig 11. False color images of peacock eyespots for different visual models. At typical viewing distances during courtship displays, peacock eyespots have central features with brightness comparable to the surrounding rings in false color images for peafowl vision in the (A) LWS/MWS/SWS and (B) VS cone channels, as well as for dichromatic mammals (C). False color image of the model train at 2m in peafowl (D) LWS/MWS/SWS and (E) VS vision, and for (F) dichromatic mammalian vision show that the eyespots feature a darker pupil-like center.

https://doi.org/10.1371/journal.pone.0210924.g011

contrasts that should be more readily detectable by mammalian predators at close distances). A consideration of cone spectral sensitivities and feather reflectance spectra suggests two reasons for this difference. First, these yellow feathers had an overall higher reflectance than the corresponding red feathers, resulting in their having a higher brightness contrast relative to leaves. Second, yellow feather pigments reflect considerable light in the UV compared to red pigments, whereas UV reflectance is low for green plants. Yellow feathers thus stimulate both predator S and L cones, while green plants primarily stimulate the L cones, providing a mechanism for distinguishing yellow feathers from green foliage backgrounds.

These conclusions should hold for other birds with red and yellow plumage given that a wide variety of species of birds have similar color vision to the species considered here (Fig 5), and that feathers colored with carotenoid pigments have very similar reflectance spectra to the pigment psittacofulvin found in parrot feathers [37–39]. Thus, our findings indicate that many species of red and yellow feathered birds that appear conspicuous to other birds and humans may in fact be cryptic or poorly visible to predators because of background matching [31]. Our findings also have broader implications for interpreting how color cues, camouflage and possible eye mimicry appear to the majority of mammals. Trichromacy in primates has been suggested to have evolved for a variety of reasons [160], including detecting ripe fruit and immature leaves [161], breaking camouflage (e.g., during foraging for eggs) [35], sexual or social signaling [162], and predator detection [163]. Our results suggest that the evolution of trichromacy may also have provided catarrhine primates, howler monkeys and some marsupials with an advantage in detecting colorful birds, reptiles, amphibians and insects.

Visual modeling: Limitations and future directions

The largest source of uncertainty in our analysis is the lack of behaviorally-measured Weber fractions for color contrast for terrestrial carnivorans for the conditions considered here, and the relatively few species for which peak cone spectral wavelengths have been measured for carnivoran mammals. This data also would be valuable for studies that often have had to rely on human visual modeling in analyzing egg camouflage [36] and the relationship between plumage, brightness and antipredator vigilance [164]. The most relevant measures would involve behavioral tests to determine whether these mammals can detect feathered model birds when other cues (e.g., olfactory) are controlled for. Any such studies ought to be sure to use illumination sources that include UV, as well as color cues that closely match the reflectance spectra of natural objects [108].

In spite of these limitations, it is important to note several factors that indicate feathers may have even lower visual contrasts in predator vision than computed here. First, our viewing and illumination geometries were chosen to optimize color and brightness cues, but predators will encounter prey under suboptimal conditions. Second, when feathers are viewed at low illumination levels, they also are likely to have lower color and brightness contrasts [165,166] and be more blurred due to reduced visual acuity [80]. Third, since UV reflectance helps distinguish feathers from green foliage, the reduction in UV irradiance in forest shade is likely to render feathers less detectable in forest shade than in direct sunlight [167]. Fourth, we also modeled only distance-dependent blurring due to visual acuity (retinal sampling), but a more complete treatment would use each species' behaviorally measured contrast sensitivity function (CSF) [80] to account for the optics of the eye and other factors that have been determined for our study species [168]. While we lacked the data to perform this additional analysis, the additional blurring would make dichromatic predators even less likely to be able to detect the feathers than our estimated contrasts indicate. Fifth, we chose to compare feathers with relatively dark green leaves (S3 Fig). The small variation in color contrasts measured between leaves with

varying shades of green indicates our findings are generalizable. The variation in brightness contrasts between leaves suggests that bright feathers should be even less visible against light green foliage. Thus, our results may overestimate the detectability of these feathers by dichromatic mammals.

It is also worth considering why these models predict that dichromatic predators and birds perceive plumage color so differently. Ultraviolet vision per se does not result in these differing visual signals: these dichromatic mammalian predators have similar near-UV S cone spectral sensitivity to the VS cones of birds [55,169]. Indeed, as noted above, since red and yellow parrot feathers and the central patches on peacock feathers reflect appreciable UV light this may make these feathers more detectable by dichromats. It is therefore important to include UV reflectance in modeling of visual signals in dichromatic mammalian visual systems, as opposed to relying on image processing of human visible RGB photographs (Pongrácz et al. 2017). These results also are not merely a consequence of birds having more types of cones than carnivores: given the similar spectral response of dichromatic mammal S and L cones and avian VS and MWS cones, color patches could in principle generate similar contrasts in both visual systems. Instead, these feathers have low contrast in dichromatic mammal vision due to a combination of low visual acuity, higher receptor noise levels and poorer spectral discrimination over the L cone response range.

Conclusion

Darwin stated that "Even the bright colors of many male birds cannot fail to make them conspicuous to their enemies of all kinds" [2]. On the contrary, our study implies that some species of birds that appear vividly colorful to humans and other birds may appear drab and inconspicuous in the eyes of mammalian predators. This conclusion is consistent with our review of the literature on predation by wild felids and canids on peafowl and other birds. The detectability of colorful plumage by predator vision depends on specifics of pigmentation, photoreceptor response, and environmental context, as suggested by sensory drive theory [170]. Thus, the predation risk incurred by colorful plumage needs to be assessed on a case-by-case basis using behavioral studies in combination with measurements of visual signals for the predator of interest.

Predators have a variety of other means of detecting prey, including visual motion perception and sensing acoustic, tactile and olfactory cues. Our results highlight the importance of understanding how dynamic behaviors during multimodal displays, foraging and other activities make birds more apparent to mammals and other predators than do their seemingly-conspicuous colors alone.

Supporting information

S1 Appendix. Predation on wild Indian peafowl.
(DOCX)

S2 Appendix. Sources of images used for textural analysis of photographs of live Indian peacock trains photographed in native habitats.
(DOCX)

S3 Appendix. Species of plants used for background foliage in multispectral images.
(DOCX)

S4 Appendix. Methods for spatially filtering multispectral images to account for visual acuity effects at varying viewing distances.
(DOCX)

S1 Fig. Multispectral camera specifications: Image sensor spectral response and filter transmission spectra.
(DOCX)

S2 Fig. Reflectance spectroscopy apparatus and multispectral camera filming setup.
(DOCX)

S3 Fig. Various green leaves imaged and analyzed for comparison with feather samples and the saucer magnolia leaves used as a background.
(DOCX)

S4 Fig. Model train false color images.
(DOCX)

S5 Fig. Model peacock train edge detected images.
(DOCX)

S6 Fig. Pattern analysis of peacocks photographed against native foliage.
(DOCX)

S1 Dataset. Color and brightness contrast data and PERMANOVA pseudo-F and P values for Indian peacock eyespot feathers.
(CSV)

S2 Dataset. Color and brightness contrast data and PERMANOVA pseudo-F and P values for model Indian peacock train.
(CSV)

S3 Dataset. Color and brightness contrast data and PERMANOVA pseudo-F and P values for Indian peacock blue body feathers.
(CSV)

S4 Dataset. Color and brightness contrast data and PERMANOVA pseudo-F and P values for parrot feathers.
(CSV)

S5 Dataset. Granularity and edge-detection visual texture data for model Indian peacock train.
(CSV)

Acknowledgments

We wish to thank Cassie Stoddard for providing us with her edge detection code, Charles Chubb and Roger Hanlon for their granularity code, and Robert Beyer for instrumentation design.

Author Contributions

Conceptualization: Suzanne Amador Kane, Roslyn Dakin.

Data curation: Suzanne Amador Kane, Yuchao Wang.

Formal analysis: Suzanne Amador Kane, Yuchao Wang.

Investigation: Suzanne Amador Kane, Yuchao Wang, Rui Fang, Yabin Lu.

Methodology: Suzanne Amador Kane, Yuchao Wang, Rui Fang, Yabin Lu.

Software: Suzanne Amador Kane, Yuchao Wang.

Validation: Suzanne Amador Kane, Yuchao Wang.

Visualization: Suzanne Amador Kane, Yuchao Wang, Rui Fang, Yabin Lu.

Writing – original draft: Suzanne Amador Kane.

Writing – review & editing: Suzanne Amador Kane, Yuchao Wang, Rui Fang, Yabin Lu, Roslyn Dakin.

References

1. Andersson MB. Sexual selection. Princeton University Press; 1994.
2. Darwin C. The descent of man and selection in relation to sex. Murray; 1888.
3. Jabr F. How beauty is making scientists rethink evolution. New York Times Magazine. 2 Jan 2019: 22–48.
4. Ranjith V, Jose B. Habitat preference of Indian peafowl (Pavo cristatus) in selected areas of Palakkad district, Kerala, India. Current Science. 2016; 110: 2177–2182.
5. Zahavi A. Mate selection—A selection for a handicap. Journal of Theoretical Biology. 1975; 53: 205–214. https://doi.org/10.1016/0022-5193(75)90111-3 PMID: 1195756
6. Endler JA. Natural Selection on Color Patterns in Poecilia Reticulata. Evolution. 1980; 34: 76–91. https://doi.org/10.1111/j.1558-5646.1980.tb04790.x PMID: 28563214
7. Møller AP, Erritzøe J, Nielsen JT. Causes of interspecific variation in susceptibility to cat predation on birds. Chinese Birds. 2010; 1: 97–111.
8. Cain KE, Hall ML, Medina I, Leitao AV, Delhey K, Brouwer L, et al. Conspicuous Plumage Does Not Increase Predation Risk: A Continent-Wide Test Using Model Songbirds. The American Naturalist. 2019; 193: 359–372. https://doi.org/10.1086/701632 PMID: 30794446
9. Munson ES. How Birds use Conspicuous Plumage to Elude Predators. The Passenger Pigeon. 1990; 52: 311–314.
10. Ruiz-Rodríguez M, Avilés JM, Cuervo JJ, Parejo D, Ruano F, Zamora-Muñoz C, et al. Does avian conspicuous colouration increase or reduce predation risk? Oecologia. 2013; 173: 83–93. https://doi.org/10.1007/s00442-013-2599-6 PMID: 23386048
11. Outomuro D, Söderquist L, Johansson F, Ödeen A, Nordström K. The price of looking sexy: visual ecology of a three-level predator–prey system. Functional Ecology. 2017; 31: 707–718. https://doi.org/10.1111/1365-2435.12769
12. Loss S, Will T, Marra P. Direct mortality of birds from anthropogenic causes. Annual Review of Ecology, Evolution, and Systematics. 2015; 46: 99–120.
13. Cronin TW, Johnsen S, Marshall NJ, Warrant EJ. Visual Ecology. Princeton University Press; 2014.
14. Endler JA, Thery M. Interacting Effects of Lek Placement, Display Behavior, Ambient Light, and Color Patterns in Three Neotropical Forest-Dwelling Birds. The American Naturalist. 1996; 148: 421–452. https://doi.org/10.1086/285934
15. Miller PE, Murphy CJ. Vision in dogs. Journal-American Veterinary Medical Association. 1995; 207: 1623–1634.
16. Håstad O, Victorsson J, Ödeen A. Differences in color vision make passerines less conspicuous in the eyes of their predators. PNAS. 2005; 102: 6391–6394. https://doi.org/10.1073/pnas.0409228102 PMID: 15851662
17. Théry M, Debut M, Gomez D, Casas J. Specific color sensitivities of prey and predator explain camouflage in different visual systems. Behav Ecol. 2005; 16: 25–29. https://doi.org/10.1093/beheco/arh130
18. Endler JA. Interactions between predator and prey. Behavioural ecology. 1991; 169–202.
19. Chiao C-C, Wickiser JK, Allen JJ, Genter B, Hanlon RT. Hyperspectral imaging of cuttlefish camouflage indicates good color match in the eyes of fish predators. PNAS. 2011; 108: 9148–9153. https://doi.org/10.1073/pnas.1019090108 PMID: 21576487
20. Nokelainen O, Hubbard N, Lown AE, Wood LE, Stevens M. Through predators' eyes: phenotype–environment associations in shore crab coloration at different spatial scales. Biol J Linn Soc. 2017; 122: 738–751. https://doi.org/10.1093/biolinnean/blx101

21. Sumner P, Mollon JD. Colors of primate pelage and skin: Objective assessment of conspicuousness. American Journal of Primatology. 2003; 59: 67–91. https://doi.org/10.1002/ajp.10066 PMID: 12619048

22. Loyau A, Gomez D, Moureau B, Théry M, Hart NS, Jalme MS, et al. Iridescent structurally based coloration of eyespots correlates with mating success in the peacock. Behav Ecol. 2007; 18: 1123–1131. https://doi.org/10.1093/beheco/arm088

23. Dakin R, Montgomerie R. Eye for an eyespot: how iridescent plumage ocelli influence peacock mating success. Behav Ecol. 2013; 24: 1048–1057. https://doi.org/10.1093/beheco/art045

24. Dakin R, Montgomerie R. Peacocks orient their courtship displays towards the sun. Behav Ecol Sociobiol. 2009; 63: 825–834. https://doi.org/10.1007/s00265-009-0717-6

25. Freeman AR, Hare JF. Infrasound in mating displays: a peacock's tale. Animal Behaviour. 2015; 102: 241–250. https://doi.org/10.1016/j.anbehav.2015.01.029

26. Dakin R, McCrossan O, Hare JF, Montgomerie R, Kane SA. Biomechanics of the peacock's display: How feather structure and resonance influence multimodal signaling. PLOS ONE. 2016; 11: e0152759. https://doi.org/10.1371/journal.pone.0152759 PMID: 27119380

27. Yorzinski JL, Patricelli GL, Babcock JS, Pearson JM, Platt ML. Through their eyes: selective attention in peahens during courtship. Journal of Experimental Biology. 2013; 216: 3035–3046. https://doi.org/10.1242/jeb.087338 PMID: 23885088

28. Petrie M, Tim H, Carolyn S. Peahens prefer peacocks with elaborate trains. Animal Behaviour. 1991; 41: 323–331. https://doi.org/10.1016/S0003-3472(05)80484-1

29. Harikrishnan S, Vasudevan K, Sivakumar K. Behavior of Indian peafowl Pavo cristatus Linn. 1758 during the mating period in a natural population. The Open Ornithology Journal. 2010; 3: 13–19.

30. Yoshioka S, Kinoshita S. Effect of macroscopic structure in iridescent color of the peacock feathers. Forma-Tokyo. 2002; 17: 169–181.

31. Stevens M, Merilaita S. Animal Camouflage: Mechanisms and Function. Cambridge University Press; 2011.

32. Stoddard MC, Stevens M. Pattern mimicry of host eggs by the common cuckoo, as seen through a bird's eye. Proceedings of the Royal Society of London B: Biological Sciences. 2010; rspb20092018. https://doi.org/10.1098/rspb.2009.2018 PMID: 20053650

33. Akkaynak D, Siemann LA, Barbosa A, Mäthger LM. Changeable camouflage: how well can flounder resemble the colour and spatial scale of substrates in their natural habitats? Royal Society Open Science. 2017; 4: 160824. https://doi.org/10.1098/rsos.160824 PMID: 28405370

34. Barbosa A, Mäthger LM, Buresch KC, Kelly J, Chubb C, Chiao C-C, et al. Cuttlefish camouflage: The effects of substrate contrast and size in evoking uniform, mottle or disruptive body patterns. Vision Research. 2008; 48: 1242–1253. https://doi.org/10.1016/j.visres.2008.02.011 PMID: 18395241

35. Troscianko J, Wilson-Aggarwal J, Griffiths D, Spottiswoode CN, Stevens M. Relative advantages of dichromatic and trichromatic color vision in camouflage breaking. Behav Ecol. 2017; 28: 556–564. https://doi.org/10.1093/beheco/arw185 PMID: 29622920

36. Stoddard MC, Kupán K, Eyster HN, Rojas-Abreu W, Cruz-López M, Serrano-Meneses MA, et al. Camouflage and Clutch Survival in Plovers and Terns. Scientific Reports. 2016; 6: 32059. https://doi.org/10.1038/srep32059 PMID: 27616020

37. McGraw KJ, Nogare MC. Distribution of unique red feather pigments in parrots. Biology Letters. 2005; 1: 38–43. https://doi.org/10.1098/rsbl.2004.0269 PMID: 17148123

38. Shawkey MD, Hill GE. Carotenoids need structural colours to shine. Biology Letters. 2005; 1: 121–124. https://doi.org/10.1098/rsbl.2004.0289 PMID: 17148144

39. Toral GM, Figuerola J, Negro JJ. Multiple ways to become red: Pigment identification in red feathers using spectrometry. Comparative Biochemistry and Physiology Part B: Biochemistry and Molecular Biology. 2008; 150: 147–152. https://doi.org/10.1016/j.cbpb.2008.02.006 PMID: 18378172

40. Dalrymple RL, Hui FKC, Flores-Moreno H, Kemp DJ, Moles AT. Roses are red, violets are blue–so how much replication should you do? An assessment of variation in the colour of flowers and birds. Biol J Linn Soc. 2015; 114: 69–81. https://doi.org/10.1111/bij.12402

41. Dakin R, Montgomerie R. Peahens prefer peacocks displaying more eyespots, but rarely. Animal Behaviour. 2011; 82: 21–28. https://doi.org/10.1016/j.anbehav.2011.03.016

42. Gokula V. Display behaviour of Indian Peafowl Pavo cristatus (Aves: Galliformes) during the mating season in viralimalai, TamilNadu, India. TAPROBANICA: The Journal of Asian Biodiversity. 2015; 7.

43. Sharma IK. Ecological Studies of the Plumes of the Peacock (Pavo cristatus). The Condor. 1974; 76: 344–346. https://doi.org/10.2307/1366352

44. Beebe W. A Monograph of the Pheasants [Internet]. Witherby & Co; 1918. https://www.jstor.org/stable/4072814

45. Gates DM, Keegan HJ, Schleter JC, Weidner VR. Spectral Properties of Plants. Appl Opt, AO. 1965; 4: 11–20. https://doi.org/10.1364/AO.4.000011

46. Jensen JR. Remote sensing of the environment: An earth resource perspective 2/e. Pearson Education India; 2009.

47. Regan B. C., Julliot C., Simmen B., Viénot F., Charles–Dominique P., Mollon J. D. Fruits, foliage and the evolution of primate colour vision. Philosophical Transactions of the Royal Society of London Series B: Biological Sciences. 2001; 356: 229–283. https://doi.org/10.1098/rstb.2000.0773 PMID: 11316480

48. Jeganathan C, Dash J, Atkinson PM. Mapping the phenology of natural vegetation in India using a remote sensing-derived chlorophyll index. International Journal of Remote Sensing. 2010; 31: 5777–5796. https://doi.org/10.1080/01431161.2010.512303

49. Lee DW. Canopy dynamics and light climates in a tropical moist deciduous forest in India. Journal of Tropical Ecology. 1989; 5: 65–79. https://doi.org/10.1017/S0266467400003229

50. Hart NS. Vision in the peafowl (Aves: Pavo cristatus). Journal of Experimental Biology. 2002; 205: 3925–3935. PMID: 12432014

51. Spitschan M, Aguirre GK, Brainard DH, Sweeney AM. Variation of outdoor illumination as a function of solar elevation and light pollution. Scientific Reports. 2016; 6: 26756. https://doi.org/10.1038/srep26756 PMID: 27272736

52. Hart NS, Partridge JC, Cuthill IC, Bennett ATD. Visual pigments, oil droplets, ocular media and cone photoreceptor distribution in two species of passerine bird: the blue tit (Parus caeruleus L.) and the blackbird (Turdus merula L.). J Comp Physiol A. 2000; 186: 375–387. https://doi.org/10.1007/s003590050437 PMID: 10798725

53. Troscianko J, Stevens M. Image calibration and analysis toolbox–a free software suite for objectively measuring reflectance, colour and pattern. Methods in Ecology and Evolution. 2015; 6: 1320–1331. https://doi.org/10.1111/2041-210X.12439 PMID: 27076902

54. Lind O, Chavez J, Kelber A. The contribution of single and double cones to spectral sensitivity in budgerigars during changing light conditions. J Comp Physiol A. 2014; 200: 197–207. https://doi.org/10.1007/s00359-013-0878-7 PMID: 24366429

55. Douglas RH, Jeffery G. The spectral transmission of ocular media suggests ultraviolet sensitivity is widespread among mammals. Proceedings of the Royal Society of London B: Biological Sciences. 2014; 281: 20132995. https://doi.org/10.1098/rspb.2013.2995 PMID: 24552839

56. Guenther E, Zrenner E. The spectral sensitivity of dark- and light-adapted cat retinal ganglion cells. J Neurosci. 1993; 13: 1543–1550. https://doi.org/10.1523/JNEUROSCI.13-04-01543.1993 PMID: 8463834

57. Jacobs GH, Deegan JF, Crognale MA, Fenwick JA. Photopigments of dogs and foxes and their implications for canid vision. Visual Neuroscience. 1993; 10: 173–180. https://doi.org/10.1017/S0952523800003291 PMID: 8424924

58. Clark DL, Clark RA. Neutral point testing of color vision in the domestic cat. Experimental Eye Research. 2016; 153: 23–26. https://doi.org/10.1016/j.exer.2016.10.002 PMID: 27720709

59. Neitz J, Geist T, Jacobs GH. Color vision in the dog. Visual Neuroscience. 1989; 3: 119–125. https://doi.org/10.1017/S0952523800004430 PMID: 2487095

60. Kasparson AA, Badridze J, Maximov VV. Colour cues proved to be more informative for dogs than brightness. Proceedings of the Royal Society of London B: Biological Sciences. 2013; 280: 20131356. https://doi.org/10.1098/rspb.2013.1356 PMID: 23864600

61. Osorio D, Vorobyev M. Photoreceptor spectral sensitivities in terrestrial animals: adaptations for luminance and colour vision. Proceedings of the Royal Society of London B: Biological Sciences. 2005; 272: 1745–1752. https://doi.org/10.1098/rspb.2005.3156 PMID: 16096084

62. Calderone JB, Jacobs GH. Spectral properties and retinal distribution of ferret cones. Visual Neuroscience. 2003; 20: 11–17. https://doi.org/10.1017/S0952523803201024 PMID: 12699079

63. Azlan JM, Sharma DSK. The diversity and activity patterns of wild felids in a secondary forest in Peninsular Malaysia. Oryx. 2006; 40: 36–41. https://doi.org/10.1017/S0030605306000147

64. Carter N, Jasny M, Gurung B, Liu J. Impacts of people and tigers on leopard spatiotemporal activity patterns in a global biodiversity hotspot. Global Ecology and Conservation. 2015; 3: 149–162. https://doi.org/10.1016/j.gecco.2014.11.013

65. Di Bitetti MS, De Angelo CD, Di Blanco YE, Paviolo A. Niche partitioning and species coexistence in a Neotropical felid assemblage. Acta Oecologica. 2010; 36: 403–412. https://doi.org/10.1016/j.actao.2010.04.001

66. Hernández-SaintMartín AD, Rosas-Rosas OC, Palacio-Núñez J, Tarango-Arámbula LA, Clemente-Sánchez F, Hoogesteijn AL. Activity patterns of jaguar, puma and their potential prey in San Luis Potosi, Mexico. ACTA ZOOLÓGICA MEXICANA (NS). 2013; 29: 520–533.

67. Kamler JF, Johnson A, Vongkhamheng C, Bousa A. The diet, prey selection, and activity of dholes (Cuon alpinus) in northern Laos. J Mammal. 2012; 93: 627–633. https://doi.org/10.1644/11-MAMM-A-241.1

68. Karanth KU, Sunquist ME. Behavioural correlates of predation by tiger (Panthera tigris), leopard (Panthera pardus) and dhole (Cuon alpinus) in Nagarahole, India. Journal of Zoology. 2000; 250: 255–265.

69. Lynam AJ, Jenks KE, Tantipisanuh N, Chutipong W, Ngoprasert D, Gale GA, et al. Terrestrial activity patterns of wild cats from camera-trapping. Raffles Bulletin of Zoology. 2013; 61.

70. Odden M, Wegge P. Spacing and activity patterns of leopards Panthera pardus in the Royal Bardia National Park, Nepal. wbio. 2005; 11: 145–152. https://doi.org/10.2981/0909-6396(2005)11[145:SAAPOL]2.0.CO;2

71. Horn JA, Mateus-Pinilla N, Warner RE, Heske EJ. Home range, habitat use, and activity patterns of free-roaming domestic cats. The Journal of Wildlife Management. 2011; 75: 1177–1185. https://doi.org/10.1002/jwmg.145

72. Sunquist M, Sunquist F. Wild cats of the world. University of chicago press; 2002.

73. Castelló JR. Canids of the World: Wolves, Wild Dogs, Foxes, Jackals, Coyotes, and Their Relatives. Princeton University Press; 2018.

74. Lawson R, Fogarty D, Loss S. Use of visual and olfactory sensory cues by an apex predator in deciduous forests. Canadian Journal of Zoology. 2019;

75. Lawson R, Fogarty D, Loss S. Use of visual and olfactory sensory cues by an apex predator in deciduous forests. Can J Zool. 2019; https://doi.org/10.1139/cjz-2018-0134

76. Hughes NK, Price CJ, Banks PB. Predators Are Attracted to the Olfactory Signals of Prey. PLOS ONE. 2010; 5: e13114. https://doi.org/10.1371/journal.pone.0013114 PMID: 20927352

77. Kelber A, Yovanovich C, Olsson P. Thresholds and noise limitations of colour vision in dim light. Philosophical Transactions of the Royal Society B: Biological Sciences. 2017; 372: 20160065. https://doi.org/10.1098/rstb.2016.0065 PMID: 28193810

78. Khokhlova TV. Current views on vision in mammals. Biol Bull Rev. 2013; 3: 347–361. https://doi.org/10.1134/S207908641305006X

79. Kang I, Reem RE, Kaczmarowski AL, Malpeli JG. Contrast Sensitivity of Cats and Humans in Scotopic and Mesopic Conditions. Journal of Neurophysiology. 2009; 102: 831–840. https://doi.org/10.1152/jn.90641.2008 PMID: 19458146

80. Melin AD, Kline DW, Hiramatsu C, Caro T. Zebra Stripes through the Eyes of Their Predators, Zebras, and Humans. PLOS ONE. 2016; 11: e0145679. https://doi.org/10.1371/journal.pone.0145679 PMID: 26799935

81. Olsson P, Lind O, Kelber A. Chromatic and achromatic vision: parameter choice and limitations for reliable model predictions. Behav Ecol. 2017; 29: 273–282. https://doi.org/10.1093/beheco/arx133

82. Pasternak T, Merigan WH. The luminance dependence of spatial vision in the cat. Vision Research. 1981; 21: 1333–1339. https://doi.org/10.1016/0042-6989(81)90240-6 PMID: 7314518

83. Meadows MG, Morehouse NI, Rutowski RL, Douglas JM, McGraw KJ. Quantifying iridescent coloration in animals: a method for improving repeatability. Behav Ecol Sociobiol. 2011; 65: 1317–1327. https://doi.org/10.1007/s00265-010-1135-5

84. Van Wijk S, Bélisle M, Garant D, Pelletier F. A reliable technique to quantify the individual variability of iridescent coloration in birds. Journal of Avian Biology. 2016; 47: 227–234. https://doi.org/10.1111/jav.00750

85. Vukusic P, Stavenga DG. Physical methods for investigating structural colours in biological systems. Journal of The Royal Society Interface. 2009; 6: S133–S148. https://doi.org/10.1098/rsif.2008.0386.focus PMID: 19158009

86. Stevens M, Párraga CA, Cuthill IC, Partridge JC, Troscianko TS. Using digital photography to study animal coloration. Biol J Linn Soc. 2007; 90: 211–237. https://doi.org/10.1111/j.1095-8312.2007.00725.x

87. Prutchi D. Exploring Ultraviolet Photography. Amherst Media; 2016.

88. Igoe D, Parisi A, Carter B. Characterization of a Smartphone Camera's Response to Ultraviolet A Radiation. Photochemistry and Photobiology. 2013; 89: 215–218. https://doi.org/10.1111/j.1751-1097.2012.01216.x PMID: 22862556

89. Yun HS, Park SH, Kim H-J, Lee WD, Lee KD, Hong SY, et al. Use of Unmanned Aerial Vehicle for Multi-temporal Monitoring of Soybean Vegetation Fraction. Journal of Biosystems Engineering. 2016; 41: 126–137. https://doi.org/10.5307/JBE.2016.41.2.126

90. Vogt MC, Vogt ME. RESEARCH ARTICLE: Near-Remote Sensing of Water Turbidity Using Small Unmanned Aircraft Systems. Environmental Practice. 2016; 18: 18–31. https://doi.org/10.1017/S1466046615000459

91. Amlaner CJ, Ball NJ. A Synthesis of Sleep in Wild Birds. Behaviour. 1983; 87: 85–119.

92. Lang SDJ, Mann RP, Farine DR. Temporal activity patterns of predators and prey across broad geographic scales. Behav Ecol. https://doi.org/10.1093/beheco/ary133

93. Robbins CS. Effect of time of day on bird activity. Studies in Avian Biology. 1981; 6: 275–286.

94. Barreira AS, García NC, Lougheed SC, Tubaro PL. Viewing geometry affects sexual dichromatism and conspicuousness of noniridescent plumage of Swallow Tanagers (Tersina viridis). The Auk. 2016; 133: 530–543. https://doi.org/10.1642/AUK-15-170.1

95. Barnett JB, Michalis C, Scott-Samuel NE, Cuthill IC. Distance-dependent defensive coloration in the poison frog Dendrobates tinctorius, Dendrobatidae. PNAS. 2018; 115: 6416–6421. https://doi.org/10.1073/pnas.1800826115 PMID: 29866847

96. Caves EM, Johnsen S. AcuityView: An r package for portraying the effects of visual acuity on scenes observed by an animal. Methods in Ecology and Evolution. 2018; 9: 793–797. https://doi.org/10.1111/2041-210X.12911

97. Endler JA. A framework for analysing colour pattern geometry: adjacent colours. Biol J Linn Soc. 2012; 107: 233–253. https://doi.org/10.1111/j.1095-8312.2012.01937.x

98. Talha MMH, Mia MM, Momu JM. Morphometric, productive and reproductive traits of Indian peafowl (Pavo cristatus) in Bangladesh. International Journal of Development Research. 2018; 8: 19039–19043.

99. Renoult JP, Kelber A, Schaefer HM. Colour spaces in ecology and evolutionary biology. Biological Reviews. 2015; 92: 292–315. https://doi.org/10.1111/brv.12230 PMID: 26468059

100. Vorobyev M, Osorio D. Receptor noise as a determinant of colour thresholds. Proceedings of the Royal Society of London B: Biological Sciences. 1998; 265: 351–358. https://doi.org/10.1098/rspb.1998.0302 PMID: 9523436

101. Olsson P, Wilby D, Kelber A. Quantitative studies of animal colour constancy: using the chicken as model. Proc R Soc B. 2016; 283: 20160411. https://doi.org/10.1098/rspb.2016.0411 PMID: 27170714

102. Kelber A, Osorio D. From spectral information to animal colour vision: experiments and concepts. Proceedings of the Royal Society of London B: Biological Sciences. 2010; 277: 1617–1625. https://doi.org/10.1098/rspb.2009.2118 PMID: 20164101

103. Stoddard MC, Prum RO. Evolution of Avian Plumage Color in a Tetrahedral Color Space: A Phylogenetic Analysis of New World Buntings. The American Naturalist. 2008; 171: 755–776. https://doi.org/10.1086/587526 PMID: 18419340

104. Troscianko J, Wilson-Aggarwal J, Stevens M, Spottiswoode CN. Camouflage predicts survival in ground-nesting birds. Scientific Reports. 2016; 6: 19966. https://doi.org/10.1038/srep19966 PMID: 26822039

105. Kelber A. Colour in the eye of the beholder: receptor sensitivities and neural circuits underlying colour opponency and colour perception. Current Opinion in Neurobiology. 2016; 41: 106–112. https://doi.org/10.1016/j.conb.2016.09.007 PMID: 27649467

106. Olsson P, Lind O, Kelber A. Bird colour vision: behavioural thresholds reveal receptor noise. Journal of Experimental Biology. 2015; 218: 184–193. https://doi.org/10.1242/jeb.111187 PMID: 25609782

107. Hart NS. Variations in cone photoreceptor abundance and the visual ecology of birds. J Comp Physiol A. 2001; 187: 685–697. https://doi.org/10.1007/s00359-001-0240-3 PMID: 11778831

108. Stoddard MC, Miller AE, Eyster HN, Akkaynak D. I see your false colours: how artificial stimuli appear to different animal viewers. Interface Focus. 2019; 9: 20180053. https://doi.org/10.1098/rsfs.2018.0053 PMID: 30603072

109. Pretterer G, Bubna-Littitz H, Windischbauer G, Gabler C, Griebel U. Brightness discrimination in the dog. Journal of Vision. 2004; 4: 10–10. https://doi.org/10.1167/4.3.10 PMID: 15086313

110. Linberg KA, Lewis GP, Shaaw C, Rex TS, Fisher SK. Distribution of S- and M-cones in normal and experimentally detached cat retina. Journal of Comparative Neurology. 2001; 430: 343–356. https://doi.org/10.1002/1096-9861(20010212)430:3<343::AID-CNE1035>3.0.CO;2-U PMID: 11169472

111. Ahnelt PK, Schubert C, Kübber-Heiss A, Schiviz A, Anger E. Independent variation of retinal S and M cone photoreceptor topographies: A survey of four families of mammals. Visual Neuroscience. 2006; 23: 429–435. https://doi.org/10.1017/S095252380623342X PMID: 16961976

112. Mowat FM, Petersen-Jones SM, Williamson H, Williams DL, Luthert PJ, Ali RR, et al. Topographical characterization of cone photoreceptors and the area centralis of the canine retina. Mol Vis. 2008; 14: 2518–2527. PMID: 19112529

113. Lind O, Karlsson S, Kelber A. Brightness Discrimination in Budgerigars (Melopsittacus undulatus). PLOS ONE. 2013; 8: e54650. https://doi.org/10.1371/journal.pone.0054650 PMID: 23349946

114. Hodos W, Bessette BB, Macko KA, Weiss SRB. Normative data for pigeon vision. Vision Research. 1985; 25: 1525–1527. https://doi.org/10.1016/0042-6989(85)90231-7 PMID: 4090287

115. Jones CD, Osorio D. Discrimination of oriented visual textures by poultry chicks. Vision Research. 2004; 44: 83–89. https://doi.org/10.1016/j.visres.2003.08.014 PMID: 14599573

116. Maertens M, Wichmann FA. When luminance increment thresholds depend on apparent lightness. Journal of Vision. 2013; 13: 21–21. https://doi.org/10.1167/13.6.21 PMID: 23729772

117. Geisbauer G, Griebel U, Schmid A, Timney B. Brightness discrimination and neutral point testing in the horse. Can J Zool. 2004; 82: 660–670. https://doi.org/10.1139/z04-026

118. Cazetta E, Schaefer HM, Galetti M. Why are fruits colorful? The relative importance of achromatic and chromatic contrasts for detection by birds. Evol Ecol. 2009; 23: 233–244. https://doi.org/10.1007/s10682-007-9217-1

119. Fleishman LJ, Perez CW, Yeo AI, Cummings KJ, Dick S, Almonte E. Perceptual distance between colored stimuli in the lizard Anolis sagrei: comparing visual system models to empirical results. Behav Ecol Sociobiol. 2016; 70: 541–555. https://doi.org/10.1007/s00265-016-2072-8

120. Lind O. Colour vision and background adaptation in a passerine bird, the zebra finch (Taeniopygia guttata). Royal Society Open Science. 2016; 3: 160383. https://doi.org/10.1098/rsos.160383 PMID: 27703702

121. Siddiqi A, Cronin TW, Loew ER, Vorobyev M, Summers K. Interspecific and intraspecific views of color signals in the strawberry poison frog Dendrobates pumilio. Journal of Experimental Biology. 2004; 207: 2471–2485. https://doi.org/10.1242/jeb.01047 PMID: 15184519

122. Russ JC. The Image Processing Handbook [Internet]. CRC Press; 2016. https://doi.org/10.1201/b18983

123. Lovell PG, Ruxton GD, Langridge KV, Spencer KA. Egg-Laying Substrate Selection for Optimal Camouflage by Quail. Current Biology. 2013; 23: 260–264. https://doi.org/10.1016/j.cub.2012.12.031 PMID: 23333313

124. Zuiderveld K. Contrast Limited Adaptive Histogram Equalization. Graphics Gems. 1994; 474–485.

125. Lynx Promocions, S.L. Photos of Indian Peafowl (Pavo Cristatus). In: The Internet Bird Collection [Internet]. [cited 25 Feb 2019]. https://www.hbw.com/ibc/species/53521/photos?title=indian%20peafowl&uid=&sort_by=value&sort_order=DESC&items_per_page=20&page=1

126. Maia R, White TE. Comparing colors using visual models. Behav Ecol. 2018; 29: 649–659. https://doi.org/10.1093/beheco/ary017

127. Anderson MJ, Walsh DCI, Clarke KR, Gorley RN, Guerra-Castro E. Some solutions to the multivariate Behrens–Fisher problem for dissimilarity-based analyses. Australian & New Zealand Journal of Statistics. 2017; 59: 57–79. https://doi.org/10.1111/anzs.12176

128. Jones DL. FATHOM: A Matlab toolbox for ecological and oceanographic data analysis [Internet]. St. Petersburg, FL USA: College of Marine Science, University of South Florida; 2017. https://www.marine.usf.edu/research/matlab-resources/

129. de Silva PK, Santiapillai C, Dissanayake S. Some aspects of the population ecology of the blue peafowl, Pavo cristatus, in Ruhuna National Park, Sri Lanka. Journal of South Asian Natural History. 1996; 2: 113–126.

130. Mondal K, Gupta S, Qureshi Q, Sankar K. Prey selection and food habits of leopard (Panthera pardus fusca) in Sariska Tiger Reserve, Rajasthan, India. mammalia. 2011; 75: 201–205. https://doi.org/10.1515/mamm.2011.011

131. Johnsingh AJT. Large mammalian prey-predators in Bandipur. Journal of the Bombay Natural History Society. 1983; 80: 1–57.

132. Hayward MW, Jędrzejewski W, Jêdrzejewska B. Prey preferences of the tiger Panthera tigris. Journal of Zoology. 2012; 286: 221–231. https://doi.org/10.1111/j.1469-7998.2011.00871.x

133. Petrie M. Peacocks with low mating success are more likely to suffer predation. Animal Behaviour. 1992; 44: 585–586. https://doi.org/10.1016/0003-3472(92)90072-H

134. Takahashi M, Arita H, Hiraiwa-Hasegawa M, Hasegawa T. Peahens do not prefer peacocks with more elaborate trains. Animal Behaviour. 2008; 75: 1209–1219. https://doi.org/10.1016/j.anbehav.2007.10.004

135. Ali S, Ripley SD. Handbook of the Birds of India and Pakistan: Together with Those of Bangladesh, Nepal, Bhutan and Sri Lanka Volume 2: Megapodes to Crab Plover. Oxford University Press; 1981.

136. Askew GN. The elaborate plumage in peacocks is not such a drag. Journal of Experimental Biology. 2014; 217: 3237–3241. https://doi.org/10.1242/jeb.107474 PMID: 25232196

137. Trivedi P, Johnsingh AJT. Roost selection by Indian Peafowl (Pavo cristatus) in Gir Forest, India. Journal of the Bombay Natural Histroy Society. 1996; 93: 25–29.

138. Yasmin S, Yahya HSA. Group size and vigilance in Indian peafowl. Journal of the Bombay Natural History Society. 2000; 97: 425–428.

139. Thavarajah NK, Tickle PG, Nudds RL, Codd JR. The peacock train does not handicap cursorial locomotor performance. Scientific Reports. 2016; 6: 36512. https://doi.org/10.1038/srep36512 PMID: 27805067

140. Wilkinson H, Thavarajah N, Codd J. The metabolic cost of walking on an incline in the Peacock (Pavo cristatus). PeerJ. 2015; 3: e987. https://doi.org/10.7717/peerj.987 PMID: 26056619

141. Tinbergen J, Wilts BD, Stavenga DG. Spectral tuning of Amazon parrot feather coloration by psittacofulvin pigments and spongy structures. Journal of Experimental Biology. 2013; jeb.091561. https://doi.org/10.1242/jeb.091561 PMID: 24031051

142. Hart N, Hunt D. Avian visual pigments: characteristics, spectral tuning, and evolution. The American Naturalist. 2007; 169: S7–26. https://doi.org/10.1086/510141 PMID: 19426092

143. Fadzly N, Burns KC, Zuharah WF. Evaluating Frugivore-fruit Interactions Using Avian Eye Modelling. Trop Life Sci Res. 2013; 24: 31–50. PMID: 24575247

144. Montgomerie R, Lyon B, Holder K. Dirty ptarmigan: behavioral modification of conspicuous male plumage. Behav Ecol. 2001; 12: 429–438. https://doi.org/10.1093/beheco/12.4.429

145. Stuart-Fox D. Opening the "black box" of modeling animal color vision: a comment on Olsson et al. Behav Ecol. 2018; 29: 284–284. https://doi.org/10.1093/beheco/arx154

146. Pike TW. Quantifying camouflage and conspicuousness using visual salience. Methods in Ecology and Evolution. 2018; 9: 1883–1895. https://doi.org/10.1111/2041-210X.13019

147. Osorio D, Ham AD. Spectral reflectance and directional properties of structural coloration in bird plumage. Journal of Experimental Biology. 2002; 205: 2017–2027. PMID: 12089207

148. Ridley M. How the peacock got his tail. New Scientist. 1981; 91: 398–401.

149. Somppi S, Törnqvist H, Kujala MV, Hänninen L, Krause CM, Vainio O. Dogs Evaluate Threatening Facial Expressions by Their Biological Validity–Evidence from Gazing Patterns. PLOS ONE. 2016; 11: e0143047. https://doi.org/10.1371/journal.pone.0143047 PMID: 26761433

150. Stevens M, Ruxton GD. Do animal eyespots really mimic eyes? Current Zoology. 2014; 60: 26–36.

151. Yorzinski JL, Platt ML, Adams GK. Eye-spots in Lepidoptera attract attention in humans. R Soc Open Sci. 2015; 2. https://doi.org/10.1098/rsos.150155 PMID: 26543589

152. Hillgarth N. Social organization of wild peafowl in India. World Pheasant Assoc J. 1984; 9: 47–56.

153. Johnsingh AJT, Murali S. The ecology and behaviour of the Indian peafowl (Pavo cristatus) Linn. of Injar. J Bombay Nat Hist Soc. 1978; 75: 1069–1079.

154. Dookia S. Ecology and Behaviour of Indian Peafowl (Pavo cristatus) in Keoladeo National Park, Bharatpur, Rajasthan, India. International Journal of Fauna and Biological Studies. 2015; 2: 97–103.

155. Ridley MW, Lelliott AD, Rands MRW. The courtship display of feral peafowl. Journal of World Pheasant Association. 1984; 9: 57–68.

156. Hodos W, Potocki A, Ghim MM, Gaffney M. Temporal modulation of spatial contrast vision in pigeons (Columba livia). Vision Research. 2003; 43: 761–767. https://doi.org/10.1016/S0042-6989(02)00417-0 PMID: 12639602

157. Peters R, Hemmi J, Zeil J. Image motion environments: background noise for movement-based animal signals. J Comp Physiol A. 2008; 194: 441–456. https://doi.org/10.1007/s00359-008-0317-3 PMID: 18264712

158. Walther BA. Do peacocks devote maintenance time to their ornamental plumage? Time budgets of male blue peafowl Pavo cristatus. Lundiana. 2003; 4: 149–154.

159. Vehrencamp SL, Bradbury JW, Gibson RM. The energetic cost of display in male sage grouse. Animal Behaviour. 1989; 38: 885–896. https://doi.org/10.1016/S0003-3472(89)80120-4

160. Carvalho LS, Pessoa DMA, Mountford JK, Davies WIL, Hunt DM. The Genetic and Evolutionary Drives behind Primate Color Vision. Front Ecol Evol. 2017; 5. https://doi.org/10.3389/fevo.2017.00034

161. Melin AD, Kline DW, Hickey CM, Fedigan LM. Food search through the eyes of a monkey: A functional substitution approach for assessing the ecology of primate color vision. Vision Research. 2013; 86: 87–96. https://doi.org/10.1016/j.visres.2013.04.013 PMID: 23643907

162. Hiramatsu C, Melin AD, Allen WL, Dubuc C, Higham JP. Experimental evidence that primate trichromacy is well suited for detecting primate social colour signals. Proc R Soc B. 2017; 284: 20162458. https://doi.org/10.1098/rspb.2016.2458 PMID: 28615496

163. Pessoa DMA, Maia R, De A Ajuz RC, Moraes PZPMRD, Spyrides MHC, Pessoa VF. The adaptive value of primate color vision for predator detection. American Journal of Primatology. 2014; 76: 721–729. https://doi.org/10.1002/ajp.22264 PMID: 24535839

164. Pascual J, Senar JC, Domènech J. Plumage brightness, vigilance, escape potential, and predation risk in male and female Eurasian Siskins (Spinus spinus). The Auk. 2014; 131: 61–72.

165. Freitag FB, Pessoa DMA. Effect of luminosity on color discrimination of dichromatic marmosets (Callithrix jacchus). J Opt Soc Am A, JOSAA. 2012; 29: A216–A222. https://doi.org/10.1364/JOSAA.29.00A216 PMID: 22330382

166. Sicsú P, Manica LT, Maia R, Macedo RH. Here comes the sun: multimodal displays are associated with sunlight incidence. Behav Ecol Sociobiol. 2013; 67: 1633–1642. https://doi.org/10.1007/s00265-013-1574-x

167. Endler JA. The Color of Light in Forests and Its Implications. Ecological Monographs. 1993; 63: 1–27. https://doi.org/10.2307/2937121

168. Jarvis JR, Wathes CM. On the calculation of optical performance factors from vertebrate spatial contrast sensitivity. Vision Research. 2007; 47: 2259–2271. https://doi.org/10.1016/j.visres.2007.04.015 PMID: 17588633

169. Stevens M, Cuthill IC. Hidden Messages: Are Ultraviolet Signals a Special Channel in Avian Communication? BioScience. 2007; 57: 501–507. https://doi.org/10.1641/B570607

170. Cummings ME, Endler JA. 25 Years of sensory drive: the evidence and its watery bias. Curr Zool. 2018; 64: 471–484. https://doi.org/10.1093/cz/zoy043 PMID: 30108628